Alpha and beta diversities of hydrothermal vent macrofaunal communities along the southwestern Pacific back-arc basins

Camille Poitrimol, Éric Thiébaut, Cédric Boulart, Cécile Cathalot, Olivier Rouxel, Didier Jollivet, Stephane Hourdez, Marjolaine Matabos

Science of the Total Environment 967 (2025) 178694

Contents lists available at ScienceDirect

Science of the Total Environment

journal homepage: www.elsevier.com/locate/scitotenv

Alpha and beta diversities of hydrothermal vent macrofaunal communities along the southwestern Pacific back-arc basins

Camille Poitrimol [a,b,c,*], Éric Thiébaut [a], Cédric Boulart [d], Cécile Cathalot [e], Olivier Rouxel [e], Didier Jollivet [a], Stéphane Hourdez [f], Marjolaine Matabos [b]

[a] Sorbonne Université, CNRS, Station Biologique de Roscoff, UMR 7144 Adaptation et Diversité en Milieu Marin, Roscoff, France
[b] Univ Brest, Ifremer, BEEP, F-29280 Plouzané, France
[c] ArcticNet, Québec Océan, Takuvik, Département de Biologie, Université Laval, Québec, QC, Canada
[d] University of Brest, CNRS, IRD, Ifremer, LEMAR, IUEM, F-29280 Plouzané, France
[e] UMR 6538 Geo-Ocean, Ifremer, CNRS, UBO, UBS, Plouzané, France
[f] UMR8222 Laboratoire d'Ecogéochimie des Environnements Benthiques, CNRS - Sorbonne Université, Observatoire Océanologique de Banyuls, Banyuls-sur-Mer, France

HIGHLIGHTS

- Southwest Pacific vent faunal assemblages are structured at different spatial scales.
- Assemblage composition is influenced by hydrothermal fluid dilution gradient.
- Notable biogeographic division exist between western and eastern basins.
- Species replacement drives diversity changes in the region.

GRAPHICAL ABSTRACT

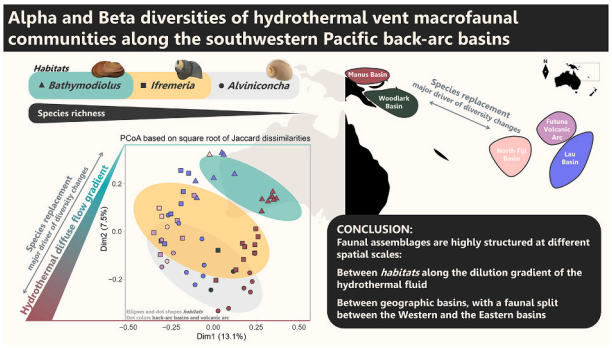

ARTICLE INFO

Editor: Olga Pantos

Keywords:
Community composition
Biodiversity partitioning
Biogeography
Vent chemistry
Bathymodiolus
Ifremeria
Alviniconcha

ABSTRACT

Ecosystems face various pressures, often leading to loss of biodiversity. Understanding how biodiversity is spatially structured, what are the driving factors, and the ecological and evolutionary processes involved is essential to assess communities' resilience to disturbances and guide efficient conservation measures. Hydrothermal vents from national waters of the West Pacific are targeted by mining industries for their mineral resources that include metals used in high-tech equipment. Although exploitation has not yet started, such activity could significantly affect ecosystem biodiversity and functioning. Here, we describe the distribution of hydrothermal biodiversity in the Southwest Pacific back-arc basins and the Futuna Volcanic Arc at different spatial scales in relation to environmental conditions and geography. We focused on three assemblages dominated by symbiotic megafauna: snails (*Alviniconcha* spp. and *Ifremeria nautilei)* and mussels (*Bathymodiolus* spp.). Faunal assemblages exhibit strong spatial structuring: between habitats along the dilution gradient of the hydrothermal fluid, and between geographic basins, with a faunal split between the Western and the Eastern basins of this region, and to a lesser extent, between fields in a basin. Species replacement along the chemical gradient drives

* Corresponding author at: Sorbonne Université, CNRS, Station Biologique de Roscoff, UMR 7144 Adaptation et Diversité en Milieu Marin, Roscoff, France.
E-mail address: camille.poitrimol@gmail.com (C. Poitrimol).

https://doi.org/10.1016/j.scitotenv.2025.178694
Received 26 September 2024; Received in revised form 24 January 2025; Accepted 29 January 2025
Available online 12 February 2025

faunal changes between *Ifremeria* and *Bathymodiolus* assemblages, while a drop in the number of species is noted when making this comparison with the *Alviniconcha* assemblage. While these local changes may result from environmental filtering along the diffuse flow gradient, geological settings and current geographic barriers, which drive colonization and speciation at larger scales, are likely shaping the vent community changes between the Eastern and Western basins. This result has significant implications for biodiversity conservation, especially in this mineral-rich setting. The Manus Basin is isolated and displays the highest proportion of endemism while the Woodlark Basin represents an important stepping-stone between the Eastern basins and Manus Basin, making them potentially highly vulnerable to mining with a risk of biodiversity loss.

1. Introduction

Understanding biodiversity and the associated drivers over space and time is a crucial step in defining better management measures to protect ecosystems. Historical ecological studies focused on biotic and abiotic factors structuring biodiversity at a local scale. However, in the last decades, a growing number of studies have focused on characterizing community assembly rules by studying changes in diversity at increasing spatial scales in order to identify the mechanisms that shape communities over time and space, and understand the relative role of historical (i.e., speciation), ecological (e.g., dispersal, environmental and biological filters) and stochastic processes (Leibold et al., 2004; Chase and Myers, 2011).

Biodiversity in space can be decomposed into local diversity (α-diversity), regional diversity (γ-diversity), and the component representing variation between communities (β-diversity) (Whittaker, 1960, 1972). Since Whittaker's seminal studies, various methods have been developed to assess β-diversity, including analyses of the dissimilarity and the underlying mechanisms in species composition between localities (Anderson et al., 2011). β-diversity patterns are mainly driven by species replacement and differences in species richness. Species replacement occurs along gradients due to environmental, historical, or biotic factors, leading to simultaneous species gains and losses (Leprieur et al., 2011). Differences in species richness can result from physical barriers to some species, fewer locally available niches or habitat degradation, with nestedness representing a specific case where species at a site are a strict subset of those at a richer site (Legendre, 2014). Understanding these patterns helps in identifying ecological processes and guiding conservation strategies (Socolar et al., 2016; Giguère and Tunnicliffe, 2021).

The Southwest Pacific back-arc basins host polymetallic sulfide deposits, resulting from hydrothermal activity, that are rich in metals of commercial interest (e.g., copper, silver and gold) and potentially strategic metals (e.g., indium, germanium) (Herzig et al., 1993; Moss et al., 2001; Evans et al., 2020). Low-temperature manganese-rich hydrothermal deposits may also contain high contents of nickel, cobalt and copper (Josso et al., 2017; Pelleter et al., 2017; Fouquet et al., 2018), making both types of deposits potential targets for deep-sea mining (Hoagland et al., 2010). Requests for permits and concessions for mining in national waters are rising, and countries need scientific advice for these authorizations. Though mining has not yet started, it could significantly impact hydrothermal communities, both directly and indirectly. Habitat destruction or fragmentation might lead to substantial biodiversity loss, depending on community resilience and potential rescue effects. Sediment plumes from mining could disrupt chemical and biological processes for vent fauna, as well as affect nearby and pelagic organisms (Boschen et al., 2013; Gollner et al., 2017; Boschen-Rose et al., 2021). In 2019, Fiji, supported by Papua New Guinea and Vanuatu, requested a 10-year moratorium to enhance understanding of hydrothermal environments and assess mining impacts (Kakee, 2020).

Benthic communities inhabiting vent systems are composed of a few, large, endemic symbiont-bearing invertebrates and a variety of smaller and numerous consumers from different trophic guilds (Van Dover, 2000; Desbruyères et al., 2006b). Symbiotic megafauna creates three-dimensional habitats, providing food and microhabitats, thereby enhancing the availability of ecological niches for smaller, mobile organisms (Govenar et al., 2005). These megafauna species are commonly used to identify different habitats or assemblages distributed along the vent fluid dilution gradient, which can be easily described from submersible observations (Sarrazin et al., 1997; Shank et al., 1998; Podowski et al., 2010). Species position themselves within this environmental gradient according to their thermo-chemical tolerances (e.g., hypoxia, fluid acidity, high temperature and hydrogen sulfide concentration) (Vismann, 1991; Bates et al., 2005), nutritional requirements (Levesque et al., 2003), and biotic interactions including predation and competition for the resources (Mullineaux et al., 2000, 2003; Henry et al., 2008). In the Southwest Pacific, three main assemblages dominated by symbiotic megafauna - the Paskentanidae snails *Alviniconcha* spp. and *Ifremeria nautilei* and the mussels *Bathymodiolus* spp. (Desbruyères et al., 1994; Collins et al., 2012) - colonize the diffuse flow gradient from moderate to lower temperature (Podowski et al., 2009, 2010). The *Alviniconcha* habitat exhibits the highest temperatures (up to 42.4 °C) and H_2S concentrations, which decrease in the *Ifremeria* and the *Bathymodiolus* habitats (up 32.5 °C to 32 °C respectively) (Podowski et al., 2010). However, little is known about the small macrofauna associated with each assemblage.

In the Southwest Pacific, hydrothermal vents are mainly located along back-arc spreading centers and volcanic arcs, including the Manus, Woodlark, North Fiji, and Lau basins, and the Feni-Tabar, Vanuatu (ex New Hebrides), Futuna, Tonga and Kermadec volcanic arcs (Desbruyères et al., 2006a; Konn et al., 2016; Boulart et al., 2022; Tunnicliffe et al., 2024), all of which are geologically recent relative to mid-oceanic ridges (< 10 million years; Hall, 2002). Although closely related to the Northwest Pacific, this region forms a biogeographic province based on vent taxa compositions (Tunnicliffe et al., 2024). Recent studies further suggest that this region is also biogeographically bisected along a west-to-east axis (Boulart et al., 2022; Poitrimol et al., 2022; Tran Lu Y et al., 2022, 2025). Unlike continuous mid-oceanic ridges that extend over thousands of kilometers, back-arc basins and volcanic arcs constitute a much more fragmented and isolated systems (Desbruyères et al., 2006a) with contrasting geological and geodynamic contexts associated with diverse tectonic structures and magma products (Hall, 2002; Schellart et al., 2006; Bézos et al., 2009). This geological diversity leads to different types of fluid chemistry and a wide variability of edifice mineralization among vents (Mottl et al., 2011; Seewald et al., 2015) that should influence species association and distribution within basins (Podowski et al., 2010; Beinart et al., 2012). Although studies have examined the distribution and composition of hydrothermal communities in the Western Pacific (Desbruyères et al., 2006a; Tunnicliffe et al., 2024), none have focused on the composition of communities associated with habitat-forming species at the scale of the whole Southwest Pacific province. Most studies focused on megafauna discarding the associated macrofauna, and were conducted at smaller spatial scales in only one or two basins, more particularly the Manus (Galkin, 1997; Collins et al., 2012), or Lau (Podowski et al., 2009, 2010; Kim and Hammerstrom, 2012; Sen et al., 2013; Diaz-Recio Lorenzo et al., 2021) and North Fiji basins (Desbruyères et al., 1994). In addition, some newly discovered vent communities have been recently described such as that of the Woodlark Ridge (south of the Manus Basin) (Boulart et al., 2022) or of the Feni-Tabar and Vanuatu arcs (Tunnicliffe

et al., 2024).

In this study, we hypothesized that the diversity of geological settings existing at different scales among the Southwest Pacific back-arc basins will lead to a great number of ecological niches, and thus a high degree of heterogeneity in the distribution of species and their assemblages. While the local conditions should structure biodiversity at small spatial scales, species histories and population connectivity should influence biodiversity at greater scales. The objective of this study is to tease apart the influence of these two main structuring factors through the description of the vent biodiversity patterns at both the regional and local scales, and investigate their associations with environmental drivers through the chemical description of the habitats of the *Alviniconcha*, *Ifremeria* and *Bathymodiolus* assemblages using a clear-cut in situ and reproducible experimental design.

2. Materials and methods

2.1. Study area and data collection

Vent community samples were collected at four back-arc basins

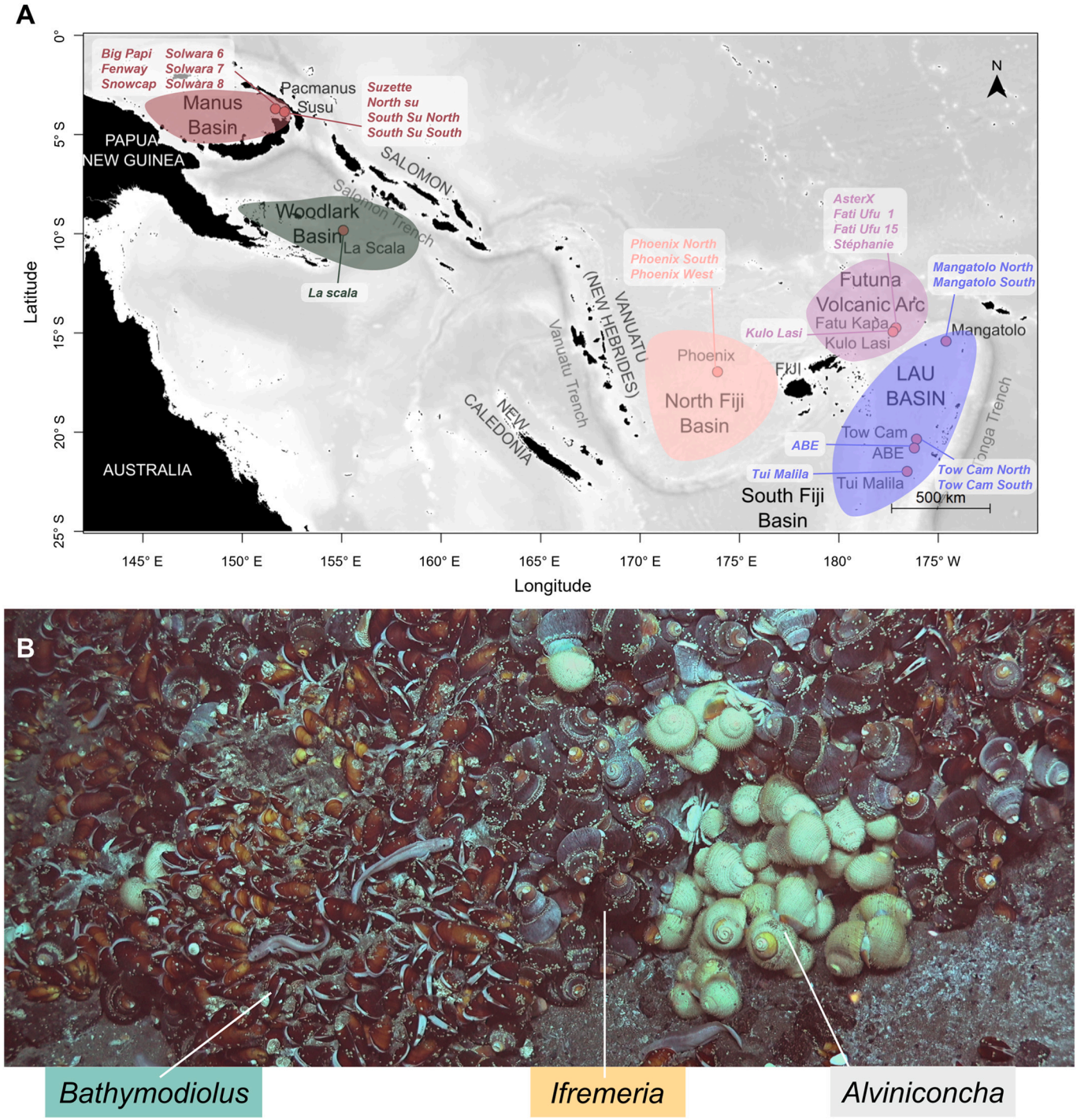

Fig. 1. Areas sampled during the CHUBACARC cruise in the Southwest Pacific (A). Colored areas represent the back-arc basins or volcanic arc sampled and red dots the sampled vent field. The sites sampled in each vent field are listed in italics. In situ photograph of the *Bathymodiolus*, *Ifremeria* and *Alviniconcha* habitats taken at the Susu hydrothermal vent field (B). Copyright Ifremer/Chubacarc 2019.

(Manus, Woodlark, North Fiji and Lau) and one volcanic arc (Futuna) in the Southwest Pacific during the CHUBACARC oceanographic cruise (March–June 2019) on board of the French Research Vessel *L'Atalante* (Hourdez and Jollivet, 2019). A hierarchical sampling was conducted including three nested spatial scales: (1) sites located a few meters to tens of meters apart, (2) fields a hundred of meters to tens of kilometers apart, and (3) basins hundreds to thousands of kilometers apart. Between one to four fields per basin, and one to six sites per field were sampled (Fig. 1A). While a clear definition of spatial scales is essential to describe biodiversity in patchy habitats such as hydrothermal vents, there is currently no consensus on a common standard to describe a vent 'site' or 'field' (Tunnicliffe, 1991; Chevaldonné and Godfroy, 1997). Recently Jamieson and Gartman (2020) defined a vent field as "a spatially associated cluster of chimneys or mounds that are linked by a common heat source and subseafloor permeability structure". But this definition can be hard to apply in the absence of knowledge on the geological features of an area. In this study, vent fields were defined according to the InterRidge Global Database of Active Submarine

Table 1
Sampling locations in the southwestern Pacific. For each sample, the following information are provided: the habitat sampled (Hab.: A, *Alviniconcha*; B, *Bathymodiolus*; I, *Ifremeria*), if the biobox sample was completed with the suction device (suction: Y, Yes; N, No), the proportion (%) of *Alviniconcha*, *Bathymodiolus* and *Ifremeria* (i.e., A, B and I) among engineer species individuals, geographical coordinates (Longitude and Latitude) and depth (m).

Basin or Volcanic Arc	Field	Site	Hab.	Sample	Suction	A	B	I	Longitude	Latitude	Depth
Manus Basin	Pacmanus	Big Papi	I	PM1	N	2	17	81	151° 40.342′E	03° 43.707′S	1703
			A	PM11	Y	100	.	.	151° 40.335′E	03° 43.731′S	1708
		Fenway	A	PM10	N	94	.	6	151° 40.373′E	03° 43.684′S	1698
			B	PM2	N	.	100	.	151° 40.370′E	03° 43.681′S	1698
			I	PM3	N	.	.	100	151° 40.367′E	03° 43.665′S	1699
			B	PM8	Y	.	100	.	151° 40.360′E	03° 43.675′S	1696
		Snow Cap	B	PM9	Y	.	83	17	151° 40.213′E	03° 43.691′S	1640
		Solwara 6	B	PM5	Y	.	99	1	151° 40.861′E	03° 43.649′S	1725
			I	PM7	Y	.	9	91	151° 40.852′E	03° 43.653′S	1729
		Solwara 7	I	PM6	Y	.	.	100	151° 40.374′E	03° 43.040′S	1769
		Solwara 8	A	PM12	Y	71	.	29	151° 40.458′E	03° 43.821′S	1737
			I	PM4	Y	18	.	82	151° 40.441′E	03° 43.825′S	1739
	Susu	North Su	B	SU1	Y	.	95	5	152° 06.060′E	03° 47.942′S	1210
			A	SU11	N	78	.	22	152° 06.046′E	03° 47.933′S	1218
			I	SU2	Y	.	.	100	152° 06.046′E	03° 47.935′S	1216
			B	SU3	Y	.	100	.	152° 06.089′E	03° 47.957′S	1195
		South Su North	A	SU10	N	96	.	4	152° 06.292′E	03° 48.497′S	1343
			I	SU4	Y	.	2	98	152° 06.291′E	03° 48.499′S	1341
			B	SU7	Y	.	100	.	152° 06.299′E	03° 48.483′S	1360
		South Su South	I	SU5	Y	5	2	93	152° 06.310′E	03° 48.583′S	1352
			B	SU6	Y	.	100	.	152° 06.310′E	03° 48.583′S	1353
			A	SU9	N	100	.	.	152° 06.309′E	03° 48.583′S	1354
		Suzette	A	SU12	N	99	.	1	152° 05.783′E	03° 47.368′S	1505
			I	SU8	Y	6	.	94	152° 05.783′E	03° 47.368′S	1506
Woodlark Basin	La Scala	La Scala	I	LS1	Y	10	.	90	155° 03.161′E	09° 47.944′S	3388
			A	LS2	N	100	.	.	155° 03.160′E	09° 47.945′S	3388
			A	LS3	N	100	.	.	155° 03.117′E	09° 47.939′S	3344
North Fiji Basin	Phoenix	Phoenix North	I	PH1	Y	2	.	98	173° 55.111′E	16° 56.936′S	1974
		Phoenix South	I	PH2	Y	1	.	99	173° 55.133′E	16° 57.005′S	1961
			B	PH3	Y	.	100	.	173° 55.127′E	16° 57.002′S	1961
			A	PH4	Y	80	.	20	173° 55.127′E	16° 57.000′S	1961
		Phoenix West	A	PH5	Y	98	.	2	173° 55.078′E	16° 56.963′S	1973
Futuna Volcanic Arc	Fatu Kapa	AsterX	I	FK1	Y	11	.	89	177° 09.134′W	14° 45.110′S	1562
			A	FK2	Y	76	.	24	177° 09.132′W	14° 45.110′S	1562
		Fati Ufu 1	A	FK6	N	84	.	16	177° 11.116′W	14° 45.597′S	1519
			I	FK8	Y	1	.	99	177° 11.113′W	14° 45.599′S	1519
		Fati Ufu 15	I	FK5	Y	2	.	98	177° 10.970′W	14° 45.326′S	1516
		Stephanie	I	FK3	N	2	.	98	177° 09.960′W	14° 44.243′S	1548
			A	FK4	N	62	.	38	177° 09.960′W	14° 44.245′S	1547
	Kulo Lasi	Kulo Lasi	I	KL1	Y	.	1	99	177° 15.551′W	14° 56.468′S	1371
Lau Basin	ABE	ABE	I	AB1	Y	2	.	98	176° 11.479′W	20° 45.784′S	2153
			B	AB2	Y	.	94	6	176° 11.480′W	20° 45.784′S	2154
			A	AB3	Y	83	.	17	176° 11.478′W	20° 45.783′S	2153
	Mangatolo	Mangatolo North	I	MG1	Y	.	.	100	174° 39.208′W	15° 24.874′S	2031
			A	MG3	Y	74	.	26	174° 39.208′W	15° 24.876′S	2031
		Mangatolo South	I	MG2	Y	7	.	93	174° 39.330′W	15° 24.958′S	2040
			A	MG4	Y	64	.	36	174° 39.331′W	15° 24.961′S	2039
	Tow Cam	Tow Cam North	I	TC1	Y	.	.	100	176° 08.203′W	20° 19.047′S	2698
			B	TC4	Y	.	100	.	176° 08.211′W	20° 19.051′S	2696
		Tow Cam South	B	TC2	Y	.	81	19	176° 08.250′W	20° 19.074′S	2711
			I	TC3	N	20	.	80	176° 08.263′W	20° 19.084′S	2711
			A	TC5	Y	87	.	13	176° 08.263′W	20° 19.085′S	2711
			A	TC6	Y	100	.	.	176° 08.258′W	20° 19.074′S	2716
			B	TC7	N	.	100	.	176° 08.261′W	20° 19.080′S	2710
	Tui Malila	Tui Malila	B	TM1	Y	8	89	3	176° 34.096′W	21° 59.352′S	1886
			B	TM2	Y	.	77	23	176° 34.088′W	21° 59.351′S	1874
			I	TM3	N	23	.	77	176° 34.098′W	21° 59.355′S	1886
			I	TM4	N	.	.	100	176° 34.094′W	21° 59.354′S	1877
			A	TM5	N	100	.	.	176° 34.091′W	21° 59.356′S	1884
			A	TM6	Y	100	.	.	176° 34.099′W	21° 59.348′S	1886

Hydrothermal Vent Fields version 3.4 (Beaulieu et al., 2013). References in the literature were used for the fields not yet registered in the database (Konn et al., 2016; Hourdez and Jollivet, 2019; Boulart et al., 2022). Sites were defined based on in situ observations and lack of activity in between. Three vent habitats located from low to high diffuse flow areas and identified according to their dominant engineer species were sampled: the *Bathymodiolus*, the *Ifremeria* and the *Alviniconcha* assemblages (Fig. 1B, Table 1, Appendix A and B). Sampling was done using the Remotely Operated Vehicle (ROV) *Victor 6000* and involved several steps: selecting the assemblage, marking the sampling area to assess the surface area sampled, taking photos and videos, performing physico-chemical measurements at three points, collecting holobiont species, and finally aspirating small fauna. Holobionts were collected using the hydraulic arm of the ROV and placed in a thermally isolated box (roughly four-five grabs). When possible, sampling was completed with a suction device to collect the associated small organisms and mobile epifauna. A total of 60 samples (biobox collections) were obtained, 42 of which included suction sampling (Table 1, see Appendix C for details).

On board, bioboxes and organisms from each dominant engineer species (e.g., *Alviniconcha*, *Ifremeria* and *Bathymodiolus*) were washed through a 250 μm sieve with filtered seawater to collect all associated fauna found on the shells or between individuals. This fauna was sorted and preserved in 96 % ethanol. In the laboratory, individuals were identified to the lowest taxonomic level possible, in general the morphospecies, using both morphological descriptions and molecular barcode data (Cytochrome Oxydase I mitochondrial gene, *Cox1*) (Annexe D; Castel et al., 2022; Poitrimol et al., 2022; Methou et al., 2023; Chabert, Hourdez, Jollivet, unpublished data). Barcode data helped confirm morphological identification and identify cryptic species, improving the taxonomic resolution and quality of our dataset (see Poitrimol et al., 2022 for gastropods). However, it was not possible to barcode all species at the scale of all sampled sites. Where several species within one taxon were known or presumed (from morphology, genetic or bibliographic data), but could not be properly distinguished morphologically nor geographically, the term 'spp.' was used.

Where precise identification was not feasible at the species level, taxa were classified at higher taxonomic levels (e.g., genus, family, order to the class or the phylum for some taxa) but were retained to maximize the amount of information. Taxonomic names were validated using the World Register of Marine Species (WoRMS) database.

2.2. Diversity analysis

Habitat-forming species were kept for the analyses. Although important in terms of biomass, they are not necessarily the most abundant in the community. In addition, several species of *Alviniconcha* and *Bathymodiolus* are known to co-occur at some vent localities, and thus of importance in estimating local diversities. Both suction and box samplers were used to assess γ-diversity. Although in most cases the addition of individuals collected with the suction device had a limited effect on local species richness estimates, few samples gained >10 species (see Appendix C). Consequently, and due to inconsistent use of the suction sampler, α- and β-diversity were estimated using only grabbed samples collected in the boxes.

2.2.1. γ-diversity

To compare γ-diversity, or regional species richness (Whittaker, 1960), between habitats and between basins/volcanic arc in the Southwest Pacific, species accumulation curves were produced with the *specaccum* function of the vegan package (Oksanen et al., 2022). Venn diagrams were constructed to measure the number of shared and unique species among the three habitats and among basins/volcanic arc.

2.2.2. α-diversity

The local diversity (α-diversity; Whittaker, 1960) was measured using different indices. 'Species' richness (SR) was calculated as the number of taxa in each sample. The expected species richness based on a rarefaction method was then estimated using the *rarefy* function and two theoretical sample sizes: 54 individuals (ES54), the smallest sample size of our dataset, and 233 individuals (ES233), which covered nearly 90 % of samples. Although this method standardizes samples sizes, it relies on assumptions that can be misleading: (1) samples are homogenous with similar numbers of individuals among species, (2) species are distributed randomly (Gray, 2000). Shannon entropy (H') and Pielou's evenness (J') indices were also calculated for each sample. Differences in species richness (SR, ES54, ES233) and Shannon and Pielou indices among the three habitats were tested using a Kruskal-Wallis test, with significant pairwise differences identified by Nemenyi and Dunn multiple comparison tests.

2.2.3. β-diversity

To analyze the variations in community composition among samples at the regional scale, a Principal Coordinate Analysis (PCoA) was performed on a species presence-absence matrix per sample, using the square root of the Jaccard dissimilarity coefficient, which avoids negative eigenvalues that could be problematic for subsequent analyses (e.g., distance-based redundancy analysis: dbRDA). This analysis was computed using the *cmdscale* function of the R package. Differences in community composition between basins, fields within a basin, sites within a field and habitats across basins were tested with a PERMANOVA test (9999 permutations) using the *adonis2* function of vegan. Habitat and basin were crossed fixed factors, with field and site as nested random factors within a basin or basin/field respectively. Pairwise differences were identified with a post-hoc PERMANOVA using the *pairwise.adonis2* function of the pairwiseAdonis package.

Two major sources of β-diversity were expected: geographic position of a given habitat and the environmental gradient between habitats from low (i.e., *Bathymodiolus* beds) to high (i.e., *Alviniconcha* clumps) diffusion areas. β-diversity was partitioned for each pair of samples into species replacement and species richness difference components using the Podani family indices with the function *beta.div.comp* of the adespatial package (Dray et al., 2022), following Legendre (2014). This was first done at the regional scale for each habitat to assess β-diversity patterns evolution along the geographic position of assemblages and then at the basin scale, to observe the evolution of β-diversity among habitats within a basin, focusing on the Manus and Lau basins because of their sufficient sample availability. Finally, species replacement, species richness difference, and similarity (*Sim*) values were displayed in SDR-simplex triangular plots (Podani and Schmera, 2011; Podani et al., 2013), showing the relative importance of similarity and dissimilarity components among sample pairs.

All analyses were performed using the R statistical software (R Core Team, 2020) with the RStudio environment (RStudio Team, 2020).

2.3. Link with the vent environment

2.3.1. Physico-chemical characterization of vent habitats

To investigate the links between environmental conditions and the associated fauna, the physico-chemical characteristics of the habitat were measured before faunal sampling. Temperature, pH and various chemical elements involved in chemoautotrophic production (Nakagawa and Takai, 2008; Dick, 2019) or potentially toxic to organisms (e.g. hydrogen sulfide, Luther et al., 2001; Le Bris et al., 2003; Matabos et al., 2008) were considered. To do so, fluids in the habitat were sampled using the PIF water sampler (adapted from sampling device described in Cotte et al. (2015)), which inlet was positioned using the ROV arm, and coupled with the ROV temperature probe. The water sampler could collect up to 30 filtered water samples in 60 ml acid clean syringes while recording the fluid temperature at 1 Hz. The water sampler was also connected to the CHEMINI in situ analyzer (Vuillemin et al., 2009) that allowed for in situ total free inorganic sulfide

measurements [ΣS(-II) = H_2S + HS^- + S^{2-}] (Poitrimol et al., 2022). Time-series measurements were performed at three locations for temperature, approximately 50 cm apart on the expected biological sampling area, with the probe positioned at about 2 cm above the surface of mussels or large gastropods to best represent the microhabitats surrounding the organisms. Three variables related to temperature were therefore calculated from the measurements: maximum (T.max), mean (T.mean) and range (T.range, expressed as the difference between the maximum and minimum temperatures). ΣS(-II) was measured at the same three locations as temperature and averaged per sample. Additionally, pH, sulfate (S(VI)), methane (CH_4), dissolved manganese (Mn) and iron (Fe) were measured on the water samples collected at one of the three locations. pH was analyzed on board using a pH electrode (Metrohm ®). Water samples were aliquoted and a fraction was poisoned using a saturated $HgCl_2$ solution and stored in crimp-sealed glass vials for on shore determination of CH_4 using the head-space method (Donval et al., 2008). Another fraction was acidified and conditioned for ICP-MS determination of total dissolved sulfur, Fe and Mn concentrations at the Pôle Océan Spectrométrie (PSO) using previously described methods (e.g., Rouxel et al., 2018). Total dissolved sulfur measured by ICP-MS is here referred to dissolved sulfate (S(VI)) since water samples were acidified to release hydrogen sulfide prior to ICP-MS analysis.

Mn was used as an indication of the dilution ratio of the hydrothermal fluid with seawater (Klinkhammer et al., 1977; Von Damm, 1990). Chemical elements mentioned above were normalized to Mn (i.e., ΣS(-II)/Mn, CH_4/Mn, S(VI)/Mn and Fe/Mn), as Mn usually behaves conservatively at these dilution ratios (Klinkhammer and Hudson, 1986; Rudnicki and Elderfield, 1992). This standardization removes the dilution factor and highlights the most reactive elements. The ΣS(-II)/Mn ratio was calculated using the ΣS(-II) value from the same point where Mn was measured. Vent fluid dilution was estimated as a percentage of the endmember Mn concentration $\%Endmember\ fluid = \frac{[Mn]_{sample}}{[Mn]_{site}} \times 100$, where $[Mn]_{Sample}$ is the Mn concentration measured in the sample and $[Mn]_{site}$ is the vent fluid endmember Mn concentration of the corresponding site, derived from measurements performed either during the CHUBACARC cruise in 2019 on vent fluid collected directly at the orifice of the chimney using Titane bottles, or from the literature (Reeves et al., 2011; James et al., 2014; Fouquet et al., 2018). Considering that pure seafloor hydrothermal fluid has zero Mg concentrations, endmember fluid Mn concentrations were calculated using a binary mixing model between endmember fluid values at Mg = 0 and seawater value. An average value was used if multiple measurements were available (see Appendix C). Each variable (raw and ratio) was tested for difference between the three habitats using a Kruskal-Wallis rank sum test, followed by Nemenyi and Dunn multiple comparison tests to identify significant pairs.

2.3.2. Environmental and spatial drivers of faunal composition

To explore the correlations between environmental or spatial variables, and species composition, a distance-based redundancy analysis (dbRDA) - an extension of the RDA proposed by Legendre and Anderson (1999) to apply a constrained ordination on data using non-Euclidean measures - was used on the square root of the Jaccard dissimilarity coefficient. Environmental variables included the three temperature variables (mean, max, range), pH, chemical element ratios to Mn, and % Endmenber fluid. Spatial variables included latitude, longitude and depth. Spearman rank correlations were calculated, and only one variable per pair was selected if its correlation coefficient exceeded 0.7 to prevent covariation. The retained variables were T.max, % Endmember fluid, Fe/Mn, ΣS(-II)/Mn, pH, depth, latitude and longitude. Samples missing one of these variables were excluded. The optimal combination of variables explaining community composition was determined by a forward selection using the *forward.sel* function of package adespatial (Dray et al., 2022). Permutation tests involving 999 random permutations were run to test the significance of canonical relationships and individual canonical axes using the *anova* function of vegan (Oksanen et al., 2022). The dbRDA was conducted using the *dbrda* function of the vegan package.

The relative influence of spatial and environmental variables on community composition was quantified through variance partitioning (Peres-Neto et al., 2006). The proportions of variance explained by environmental variables alone, spatial variables alone, and their interactions were estimated from three dbRDAs with the *varpart* function of vegan. Three matrices were used: the dissimilarity matrix of the square root of the Jaccard dissimilarity coefficient, and the environmental and spatial data from the forward selection. All testable fractions were tested with ANOVA permutation tests (999 permutations) on dbRDAs using the *anova* function of vegan (Oksanen et al., 2022).

3. Results

Alviniconcha and *Ifremeria* habitats were found at all vent fields; however, *Bathymodiolus* were absent at La Scala (Woodlark Basin), and few isolated individuals were found on chimneys in the Futuna volcanic area and in crevices at the Mangatolo vent field (North of the Lau Basin). These individuals were a mixture of *B. manusensis* and *B. septemdierum,* while only *B. manusensis* was found at Manus and only *B. septemdierum* at Lau and North Fiji. Very few mussel beds were found at Phoenix vent field (North Fiji Basin) where only one mussel patch was sampled (see Appendix B). While habitats are defined in terms of the three biomass-dominant engineer species, these species partly overlapped due to their highly patchy distribution at some locations. In samples collected from the *Alviniconcha* habitat, this taxon accounted for 62–100 % of engineer species abundances (Table 1). *Bathymodiolus* and *Ifremeria* comprised 77–100 % of the engineer species abundances in their respective habitats (Table 1). In most cases, mixing occurred between *Alviniconcha* and *Ifremeria*, with one species typically dominating depending on the habitat. No *Bathymodiolus* were collected in *Alviniconcha* samples, and only one mussel sample contained *Alviniconcha* individuals (i.e., TM1, Table 1). A mixture of the three species appeared only in three samples from *Ifremeria* and *Bathymodiolus* habitats.

3.1. Vent biodiversity distribution

A total of 132,364 individuals were sorted and distributed among 116 taxa based on their morphology and molecular *Cox1* barcoding data (Appendix D). Of these, 87 taxa were morphospecies, with 45 identified at the species level and 42 at a higher taxonomic level (taxa with 'sp.' or 'aff.' mentioned). Many taxa had very low occurrence, 28 were unique taxa (only found in one sample) and 10 were duplicate taxa (only found in two samples). Without suction-derived samples, 98 taxa (84.5 % of the sampled species) remained in the dataset (Appendix D).

3.1.1. γ-diversity

The most represented taxa in terms of species richness were polychaetes (~44 % of taxa) and gastropods (~33 %, including *Alviniconcha* and *Ifremeria* species). The remaining 23 % included arthropods (~13 %), bivalves and echinoderms (~3 % each, including *Bathymodiolus* species), nematodes, nemerteans, platyhelminths, cnidarians, solenogasters and Sipuncula (<1 % each). Some values may be underestimated, for instance copepods and nematodes were not identified at a lower taxonomic level despite different morphotypes/species being observed (see Diaz-Recio Lorenzo et al., 2023). Mollusks and annelids showed high richness considering habitats separately (Fig. 2A) or at a basin or volcanic arc scale (Fig. 2B).

'Species' accumulation curves per habitat at the regional scale did not reach an asymptote, indicating that a higher number of taxa could be recorded with increased sampling. The *Bathymodiolus* habitat was the richest in terms of number of taxa (98 taxa), followed by the *Ifremeria* habitat (78) and *Alviniconcha* habitat (61) (Fig. 3A). About 40 % of taxa were shared among the three habitats, with *Ifremeria* and *Bathymodiolus*

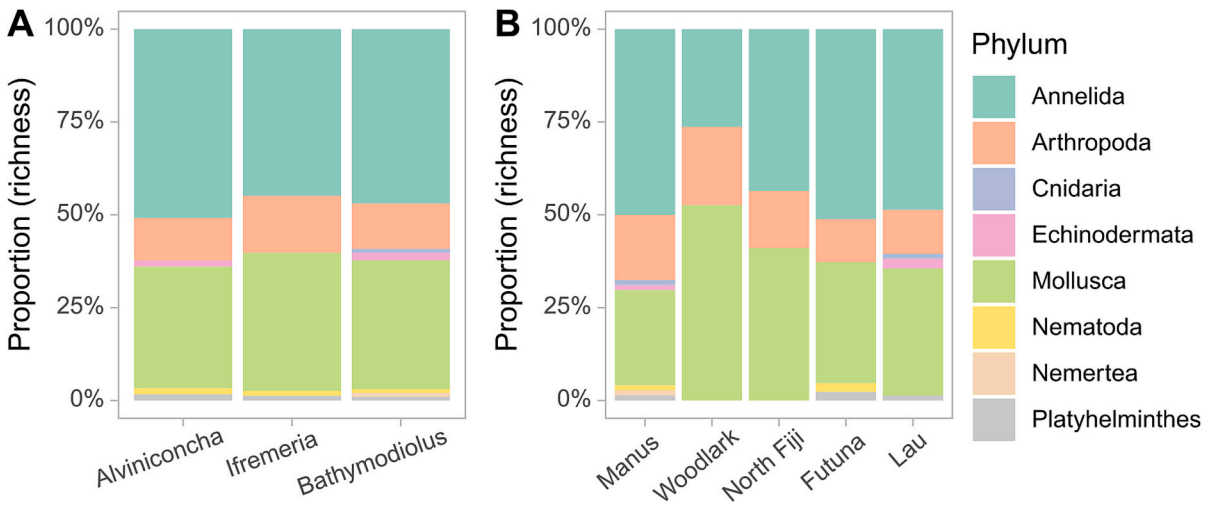

Fig. 2. Bar plot showing the phylum proportion within the *Alviniconcha*, *Ifremeria* and *Bathymodiolus* Southwest Pacific hydrothermal vent habitats (A) and within the different basins (i.e., Manus, Woodlark, North Fiji and Lau) and volcanic arc (i.e., Futuna) (B), calculated from the dataset produced using the box and suction data, and expressed in terms of richness of taxa.

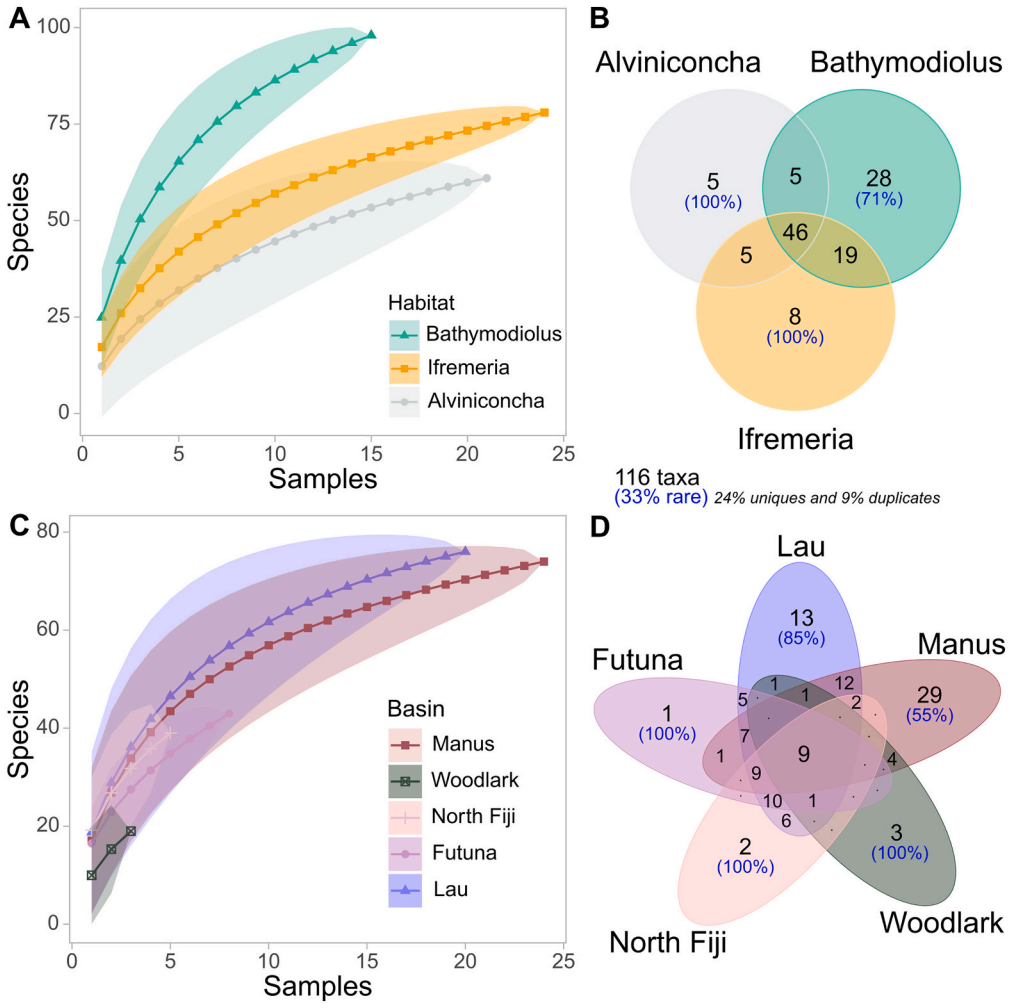

Fig. 3. Species accumulation curves (species ± SD) based on samples for three hydrothermal vent habitats from the Southwest Pacific (A), and Venn diagram showing the number of taxa shared and specific to one habitat (B). Species accumulation curves (species ± SD) based on samples for the four basins (i.e., Manus, Woodlark, North Fiji and Lau) and the one volcanic arc (i.e., Futuna) from the Southwest Pacific (C), and Venn diagram showing the number of taxa shared and specific to an area (D). For taxa unique to a habitat or area, the percentage of rare species is shown in brackets in blue.

sharing more taxa with each other than with *Alviniconcha* (Fig. 3B). A large proportion of the taxa found exclusively in a single habitat were rare (i.e., unique or duplicate taxa, Fig. 3B). Many taxa unique to a single habitat were rare, including all taxa in *Alviniconcha* and *Ifremeria*, as well as over two-thirds of those endemic to *Bathymodiolus*.

'Species' accumulation curves per basin or volcanic arc did not reach an asymptote in all the investigated areas. Species diversity was higher at the Lau and Manus basins but also resulted from a greater sampling effort. Approximately 31 % of taxa were unique to either the Eastern region (North Fiji Basin, Lau Basin, and Futuna Volcanic Arc) or the Western region (Manus Basin and Woodlark Ridge) (Fig. 3D). Over 80 % of Western taxa were exclusive to the Manus Basin, which accounted for a quarter of all sampled taxa. More than half of Manus-endemic taxa were found only in *Bathymodiolus* habitats. Only 27 % of taxa were shared between Manus and the Eastern basins plus Futuna, with a third being ubiquitous. Most unique taxa were rare, and despite limited sampling on the Woodlark Ridge, three taxa were found only there, associated with *Ifremeria*.

3.1.2. α-diversity

The number of individuals within the same habitat varied considerably among samples (Fig. 4A and Appendix C). On average, the *Ifremeria* habitat had more individuals than the *Alviniconcha* habitat (post-hoc comparisons, $p < 0.05$) (Fig. 4A).

Taxonomic richness indices also varied within habitats (Fig. 4B-D and Appendix C). These indices differed significantly between the three habitats (SR, ES54 and ES233 Kruskal-Wallis test, *p-values* < 0.05), increasing from *Alviniconcha* to *Ifremeria* and *Bathymodiolus*. *Alviniconcha* was significantly less rich than the other for ES233 and SR (post-hoc Nemenyi and Dunn test, *p-values* < 0.05).

The Shannon and Pielou indices were highly variable among samples, regardless of the habitat (Fig. 4E-F and Appendix C). While the Shannon index significantly differs between *Alviniconcha* and *Ifremeria* habitats (post-hoc Nemenyi and Dunn test, $p < 0.05$), with *Alviniconcha* showing lower diversity (Fig. 4E), Pielou's evenness did not significantly differed between habitats (Kruskal-Wallis test, $p > 0.05$). For some samples, the dominance of a few species accounted for the Shannon and Pielou indices low values.

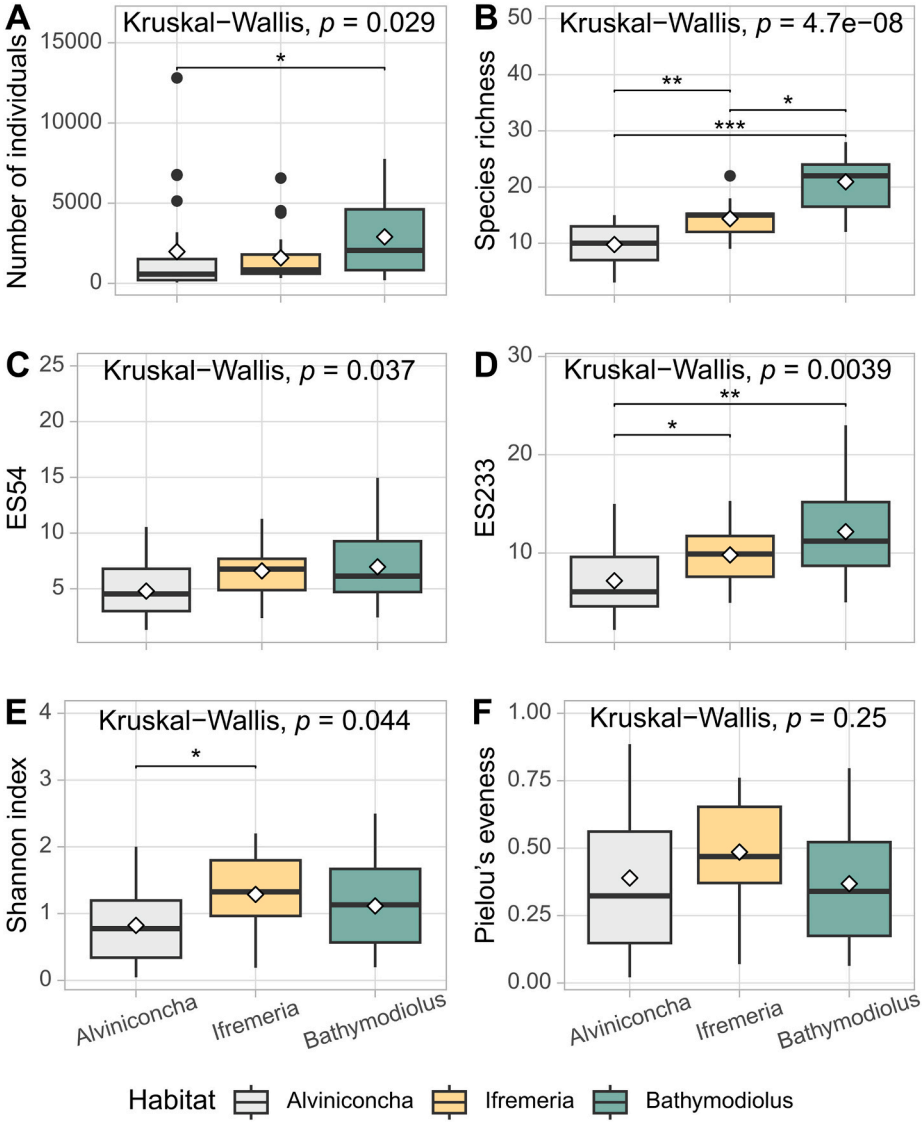

Fig. 4. Box plots of different diversity indices calculated per sample (considering the data from box only) for each of the three habitats: *Alviniconcha*, *Ifremeria* and *Bathymodiolus*. The total number of individuals (A), Species richness calculated as the number of taxa in each sample (B), the expected number of species based on 54 individuals ES54 (C) and based on 233 individuals ES233 (D), Shannon index (E) and Pielou's evenness (F) of macrofaunal communities by habitat. White rhombus indicates the average. Kruskal-Wallis test results and level of significance of the post-hoc Nemenyi and Dunn test: * p values <0.05; ** p values <0.01; *** p values <0.001.

3.1.3. β-diversity

The first two axes of the PCoA explained nearly 21 % of the species compositional variance of vent communities (Fig. 5A). These axes distinguished samples by habitat, from *Alviniconcha* to *Bathymodiolus,* and longitude, separating the Eastern basins (North Fiji, Lau, Futuna) from the Western basins (Woodlark, Manus). *Bathymodiolus* samples were well separated from the other, *Alviniconcha* and *Ifremeria* samples overlapped, suggesting a greater faunal similarity, especially in the Eastern region. Species that contributed the most to the discrimination of the samples were linked to the eastern and western separation. It included species exclusive to some basins or areas, such as species collected only in the Eastern basins (i.e., the gastropods *Symmetriapelta* spp. and the polychaetes *Branchipolynoe trifurcus*), two sibling species present at either the Manus Basin (*Lepetodrilus schrolli*) or the other Eastern basins (*Lepetodrilus fijiensis*) and, species only collected in the Manus Basin (*Lamellomphalus manusensis* and *Bathymodiolus manusensis,* although individuals of the latter have been recorded in Futuna and Mangatolo but were not part of the samples used in this study). Other species were also likely to discriminate between habitats with species found most often within mussels (i.e., the commensal scale-worms living in deep-sea mussels, gathered in the taxon *Branchipolynoe* spp. in this study), or in the *Alviniconcha* habitat (i.e., *Alviniconcha kojimai* mostly found in diffuse venting systems and absent from the PACMANUS ridge: also see Castel et al., 2022).

PERMANOVA analysis identified significant variations in species composition between basins, between habitats and considering the interaction of the two, as well as among fields within a basin (Table 2A). Fauna composition differed between the three habitats (Post-hoc pairwise comparisons *p-values* < 0.001). Assemblages from Woodlark and Manus were clearly distinct from others region. In the Eastern region, only assemblages from the Lau Basin and the Futuna Volcanic Arc differed (Table 2B). Most pairwise comparisons did not reveal significant differences between fields within a basin, likely due to limited statistical power, except for the assemblages of Mangatolo, Tow Cam, and Tui Malila, which were significantly different one to each other (*p-values* < 0.05).

Table 2
Results of the PERMANOVA analysis based on the square root of Jaccard dissimilarity to test for differences in vent macrofaunal assemblages between basins/volcanic arc and habitats (fixed factors), and field within a basin/volcanic arc and sites within a field (nested random factors (A) and *p* values results on the post-hoc pairwise basins comparison (B). Df: degrees of freedom, SS: Sum of squares, F; pseudo-F value by permutation, P: *p* values based on 9999 permutations. Significant values are highlighted in bold.

A

	Df	SS	R^2	F	P
Basin or Volcanic Arc	4	3.7979	0.17099	3.3551	**0.0001**
Habitat	2	2.2701	0.10220	4.0108	**0.0001**
Basin or Volcanic Arc*Habitat	6	2.2083	0.09942	1.3006	**0.0034**
Basin or Volcanic Arc/Field	5	1.9513	0.08785	1.3791	**0.0026**
Basin or Volcanic Arc/Field/ Site	15	4.3426	0.19552	1.0230	0.3479
Residuals	27	7.6409	0.34401		
Total	59	22.2111	1.00000		

B

	Lau Basin	Futuna Volcanic Arc	North Fiji Basin	Woodlark Basin
Futuna Volcanic Arc	**0.013**			
North Fiji Basin	0.966	0.533		
Woodlark Basin	**0.004**	**0.006**	**0.024**	
Manus Basin	**0.001**	**0.001**	**0.001**	**0.007**

At the scale of the Southwest Pacific, β-diversity partitioning showed that the *Alviniconcha* habitat had a total β-diversity of 0.36 with 60 % of species replacement and 40 % of species richness difference. *Bathymodiolus* and *Ifremeria* habitats had similar total β-diversity values (0.37 and 0.32, respectively), with higher species replacement (77 % and 76 %) and lower richness difference (23 % and 24 %). Consistent with these results, SDR-simplex approaches indicated among-samples variation dominated by species replacement for the *Ifremeria* and *Bathymodiolus*

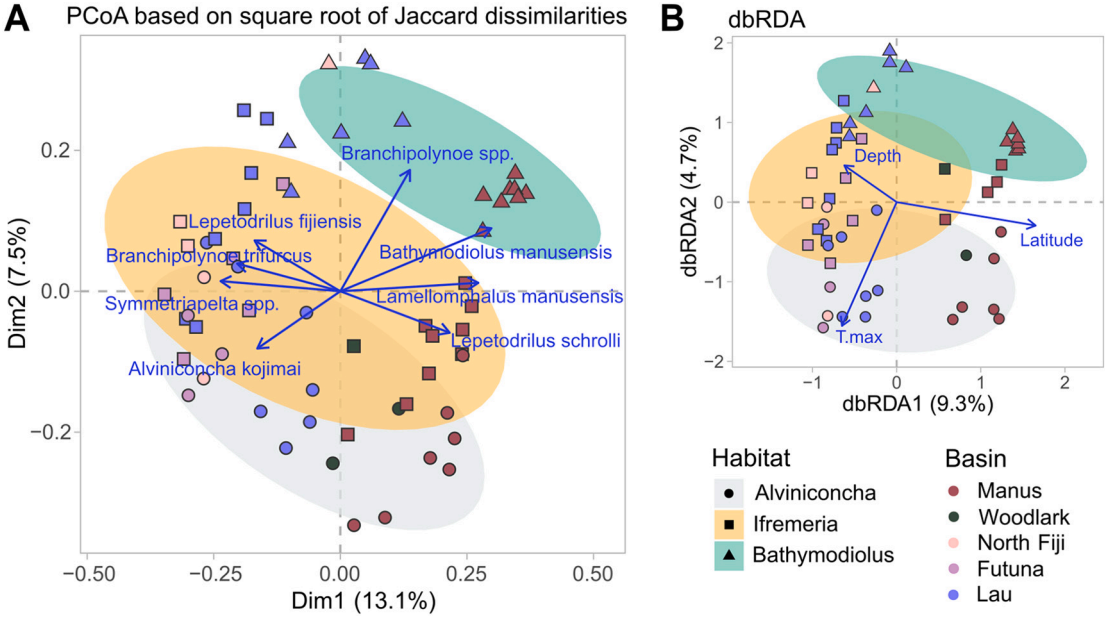

Fig. 5. Principal Coordinate Analysis (PCoA) based on the square root of the Jaccard dissimilarities representing the samples community composition variability at the regional scale and among the three different vent habitats (A). Species which had a correlation >0.6 with the first two axes were displayed in blue. Results of distance based redundancy analysis (dbRDA) based on square root of Jaccard dissimilarities and physico-chemical data (i.e., maximal temperature 'T.max') and spatial data (i.e., depth and latitude) selected by the forward selection procedure performed, excluding the suction collected data and using the ratio to manganese (Mn) for the chemical values (B). Symbol shapes and 80 % confidence ellipses represent the three different habitats, while symbol colors represent the different basins or volcanic arcs.

habitats, with mean relative values of 50 % and 57 %, respectively, whereas it was lower (43 %) for the *Alviniconcha* habitat due to a higher number of sample pairs with greater richness differences (Fig. 6). For *Alviniconcha* clumps, transition from a strong nestedness with high richness differences to a high species replacement was observed.

At a basin scale, total β-diversity was 0.37 for the Manus Basin, with 53 % species replacement and 47 % richness difference, and 0.34 for the Lau Basin, with 63 % species replacement and 37 % richness difference. SDR-simplex approaches showed among-samples variation mostly dominated by species replacement, a process more pronounced in the Lau Basin (Lau Basin: mean relative Similarity = 31.0, Repl = 43.8, RichDiff = 25.2; Manus Basin: mean relative Similarity = 26.3, Repl = 39.2, RichDiff = 34.5) (Fig. 7). The Manus Basin sample-pairs showed transitions from perfect nestedness with high richness differences to high species replacement with relatively few shared species. Variation was dominated by species richness difference when comparing samples involving *Alviniconcha* habitat (light gray, orange and dark green dots, Fig. 7), while samples involving only *Bathymodiolus* or *Ifremeria* habitats showed more balanced patterns dominated by species replacement (yellow, dark and light blue dots). Patterns were different in the Lau Basin (Fig. 7). Ecological processes involved were quite similar regardless of the type of habitat, with species replacement dominating, except for pairs comparing the *Alviniconcha* and *Bathymodiolus* habitat (dark green dots), where the effect of richness was roughly equal.

3.2. Environmental and spatial drivers of faunal composition

3.2.1. Physico-chemical conditions

Details of the environmental measurements and geographic positions are in Appendix C. Only a few environmental variables distinguished the three habitats. Temperature variables (mean, max, range) differed significantly, with higher mean and maximal temperatures in the *Alviniconcha* habitat than in the *Ifremeria* and the *Bathymodiolus* habitats (Fig. 8A and Appendix E.1). Temperature range differences were significant only between *Bathymodiolus* and the other two habitats, with smaller ranges in *Bathymodiolus* compared to *Ifremeria* and *Alviniconcha* (Appendix E.1). Mean ΣS(-II) levels differed significantly and were lower in *Bathymodiolus* than in *Alviniconcha* (Fig. 8B), but not for ΣS(-II)/Mn ratio (Fig. 8C). Conversely, no differences were observed between habitats for sulfur (S) when considering the raw data (see Appendix E.1), whereas significant differences were found for S/Mn ratio (Fig. 8D), with higher values in *Bathymodiolus* than in *Alviniconcha*. Manganese concentration (raw values) and % Endmember fluid also varied significantly, being lower in *Bathymodiolus* compared to *Alviniconcha* with *Ifremeria* values in between (Fig. 8E-F). No significant differences were found among habitats for pH, Fe/Mn, CH_4/Mn, or concentration of CH_4 and Fe (Fig. 8G-H; Appendix E.1).

3.2.2. Spatial and environmental drivers of faunal composition

Spearman rank tests showed strong correlations among temperature

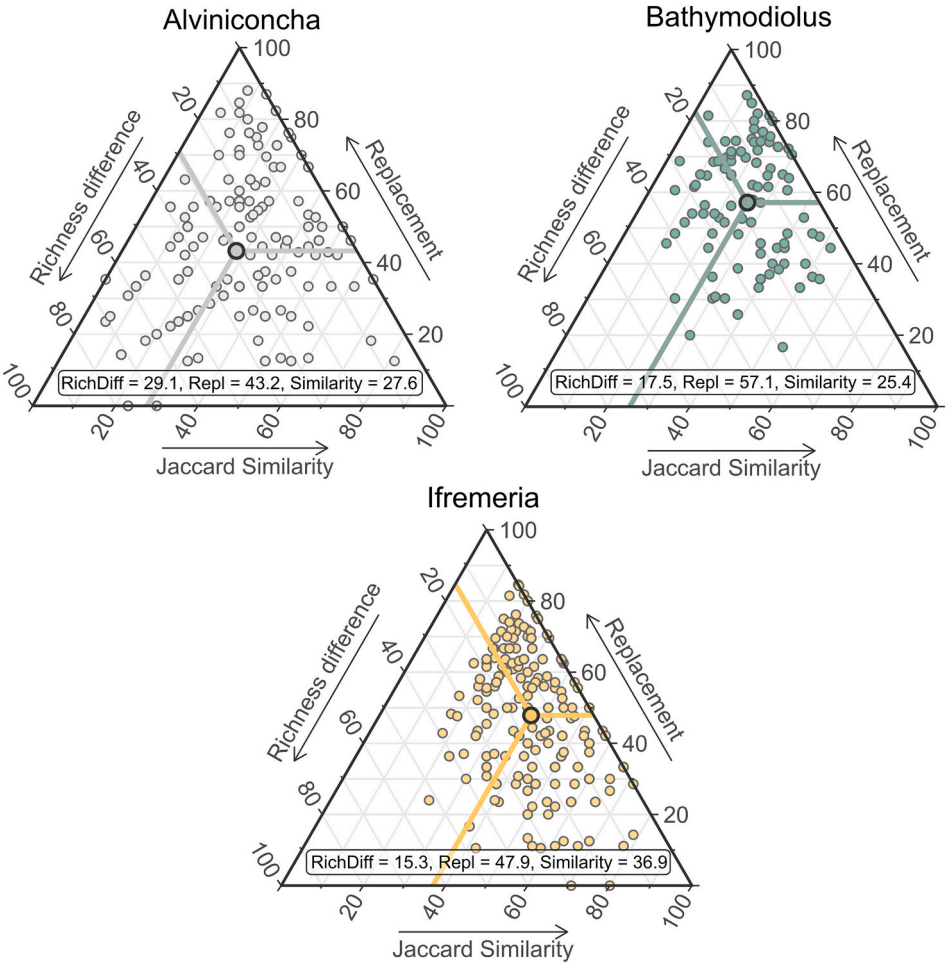

Fig. 6. SDR-simplex plots illustrating the relative importance of the Jaccard similarity and the two components of β-diversity, the species replacement and species richness difference components calculated using the Podani family indices, among all pair of samples for the three vent habitats along the Southwest Pacific geographical gradient. Each point refers to a pair of samples represented by three values: the Jaccard similarity and Podani family indices, species replacement (Repl) and species richness difference (RichDiff). Their mean values are shown in the box. The point circled in black represents the mean position of the sample pairs.

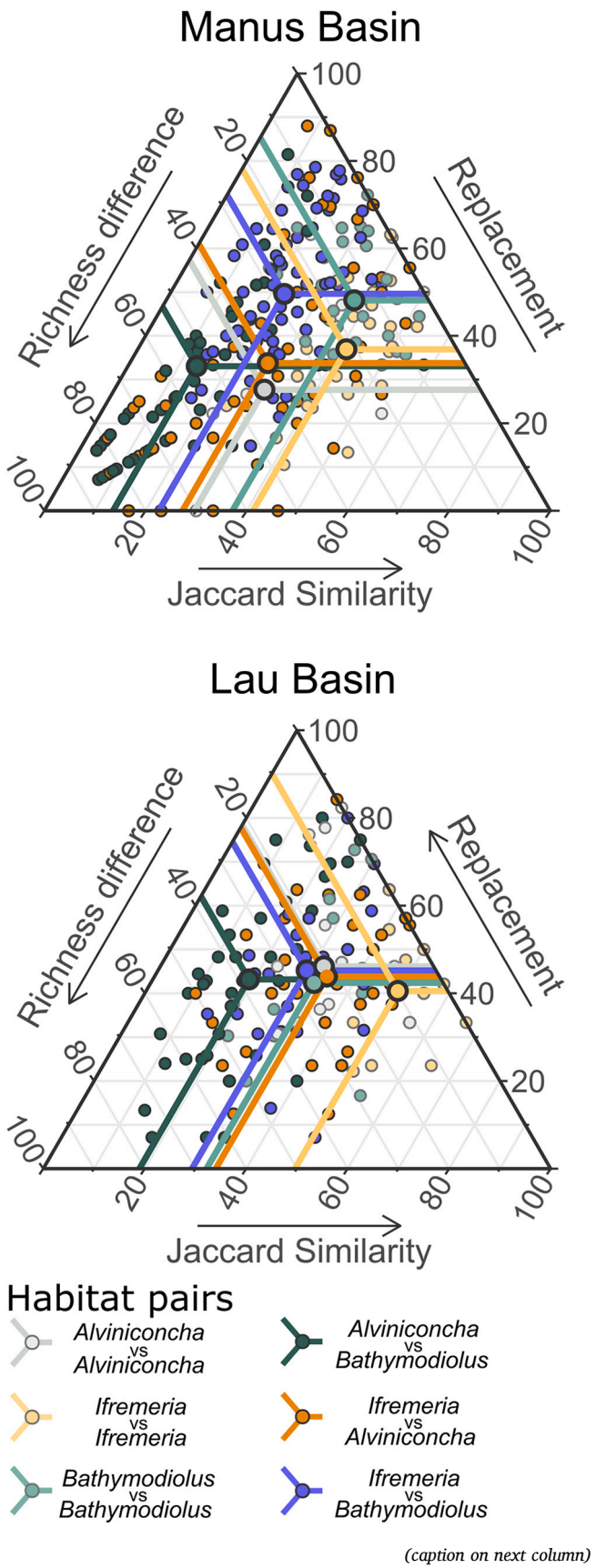

(caption on next column)

Fig. 7. SDR-simplex plots illustrating the relative importance of the Jaccard similarity and the two components of β-diversity, the species replacement and species richness difference components calculated using the Podani family indices, among all pair of samples at the scale of the Lau and Manus basins and along the vent fluid dilution gradient between the different habitats. Each point refers to a pair of samples represented by three values: the Jaccard similarity and Podani family indices, species replacement (Repl) and species richness difference (RichDiff). The different colors indicate the habitats compared in the sample pair. Larger points circled in black represents the mean position of each type of sample pairs.

variables (>0.7) and negative correlations (<−0.7) between % Endmember fluid and S/Mn and CH_4/Mn ratios (Appendix E.2). Thus, only maximum temperature, % Endmember fluid along with Fe/Mn, ΣS(-II)/Mn, pH, depth, latitude, and longitude, were used in the forward selection procedure. Due to missing data, 51 of the 60 samples were analyzed. The forward selection chose maximal temperature (T.max), depth and latitude as significant variables. A dbRDA ($p < 0.001$) using a metrix based on the square root of the Jaccard distances and these variables, explained 16.93 % of the total variance of macrofauna assemblages, with the first two axes accounting for 9.3 % and 4.7 % of the variance ($p < 0.001$) (Fig. 5B). Latitude divided eastern from western basins while maximum temperature partitioned the habitats from low (i.e., *Bathymodiolus* habitat) to moderate (i.e., *Alviniconcha* habitat) diffuse flow areas. The third axis (2.9 % of the variance, $p < 0.01$), correlated with the depth, distinguishing the Woodlark Ridge (Appendix E.3). Variance partitioning showed T.max explained 3.0 % and spatial variables (i.e., depth and latitude) 8.2 % of variance, with interactions explaining 0.4 % and residuals 88.4 %. All testable fractions were significant (*p-values* < 0.001).

4. Discussion

In this study, we assessed for the first time the γ-diversity and patterns of α- and β-diversities for vent macrofauna communities at different spatial scales within three iconic species assemblages of the Southwest Pacific. Using a set of spatial and environmental variables, we showed that faunal assemblages are highly structured along the hydrothermal diffuse flow gradient - from moderate temperatures in *Alviniconcha* habitat to low temperatures in *Bathymodiolus* habitat - and geographically separated between the Western (Manus and Woodlark Basins) and Eastern regions (Lau and North Fiji basins plus Futuna Volcanic Arc).

4.1. Faunal composition of Southwest Pacific hydrothermal vents

Quantifying and assessing local and regional biodiversity require a good taxonomic resolution, which is challenging in this region due to frequent taxonomic revisions and new species descriptions, especially following the discovery of cryptic species with molecular tools (Pearson and Rouse, 2022; Chen and Sigwart, 2023; Zhang et al., 2023; Chen et al., 2024). In addition, original taxonomic descriptions do not always mention species morphological plasticity, sex dimorphism or ontogenic changes, as descriptions are only based on a small number of individuals while morphological variability may be high (e.g., Chen et al., 2019; Chen and Watanabe, 2020). Combining morphological descriptions (morpho-species) and molecular barcoding, improved species diversity estimates. Although identifying additional species complexes could have strengthened our observed patterns, we adopted a conservative approach for some taxa with identified cryptic species to avoid creating biased patterns. We indeed lacked information at the regional scale to properly delineate their distribution and rule out the hypothesis of their co-occurrence at some locations. For instance, *Cox1* barcoding suggested cryptic species for the *Austinograea alayseae* crab (S. Hourdez, unpublish results), but available data were insufficient to assign a reliable taxon to each individual. Similarly, many polychaetes remained at the genus

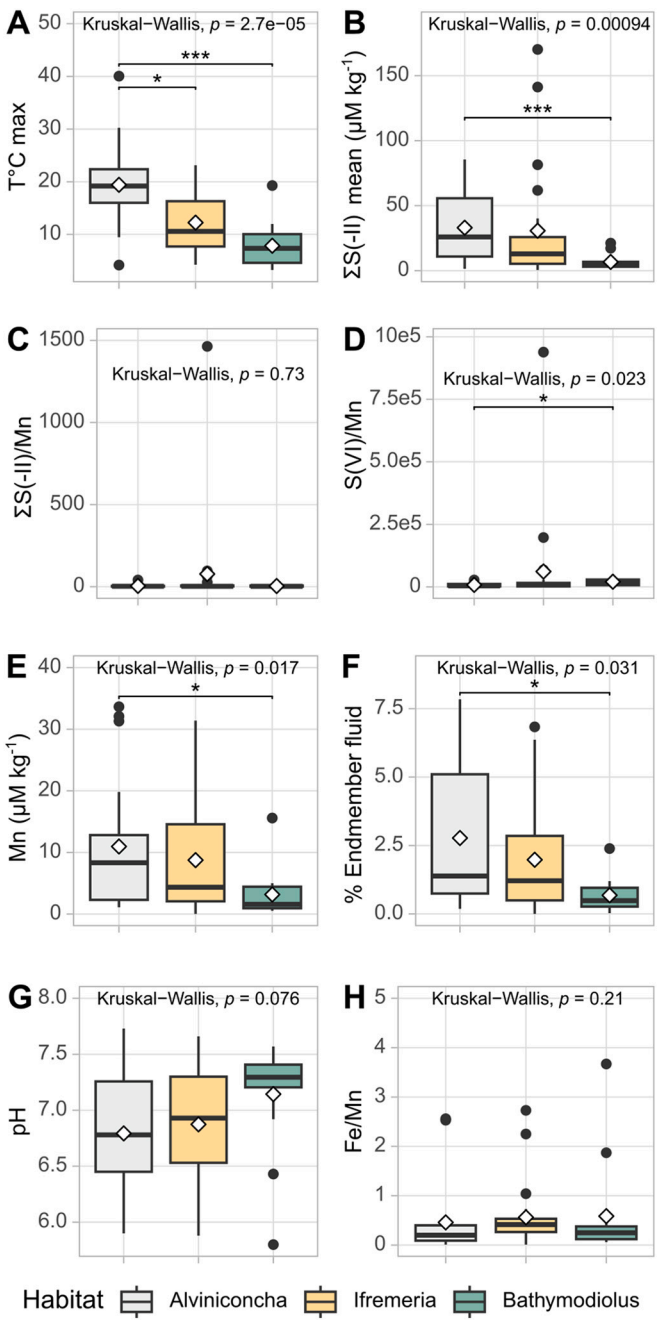

Fig. 8. Box plots of the physico-chemical measurements calculated per sample for each habitat: the maximal temperature (A), mean free inorganic sulfides [ΣS (-II) = $H_2S + HS^- + S^{2-}$] (μM kg^{-1}) (B), the ratio of free inorganic sulfides (C) and sulfate (S(VI)) (D) to manganese concentrations (Mn), raw manganese concentrations Mn (μM kg^{-1}) (E), the % Endmember fluid = [Mn]Sample/[Mn] site × 100[Mn]Sample/[Mn]site × 100, where $[Mn]_{Sample}$ is the Mn concentration (μM) measured in the sample and $[Mn]_{site}$ is the vent fluid end-member Mn concentration (μM) of the corresponding site (F), the pH (G), and the ratio of iron (Fe) to manganese concentrations (Mn) (H). White rhombus indicates the average. Kruskal-Wallis test results and level of significance of the post-hoc Nemenyi and Dunn test: * p values <0.05; ** p values <0.01; *** p values <0.001.

level although morphological identification or *Cox1* barcoding highlighted several species (S. Hourdez, NCBI Publication underway). Other polychaetes and phyla (e.g., copepods, nematodes, nemerteans) lacked sufficient genetic data or expertise for precise identification.

Although the identification for some groups remained at a low taxonomic resolution, we do not expect it to fundamentally affect the observed patterns. Indeed, Diaz-Recio Lorenzo et al. (2021) found higher copepod species richness in *Bathymodiolus* than in *Alviniconcha* habitat, in line with our results. In *Alviniconcha* habitat, *Stygiopontius lauensis*, a vent-endemic copepod, dominated copepod community and constituted over 90 % of the total abundance. Diaz-Recio Lorenzo et al. (2023) also demonstrated that the morphospecies *S. lauensis* was subdivided into five cryptic, basin-specific species, clearly contributing to community differentiation.

Using the genus or family level for some taxa probably attenuates the great faunal differences between the Eastern and Western regions, and possibly between the Manus and Woodlark basins, which clearly differ by depth. Considerable zoological work remains in the Southwest Pacific, as many species are still undescribed. Not accounting for the potentially large number of cryptic species (Poitrimol et al., 2022; Diaz-Recio Lorenzo et al., 2023), some families still have no described species for vents from this region of the world (e.g., the Capitellidae, Nereididae). This effort is essential if we expect to describe biodiversity on a regional scale and better understand the evolutionary and ecological processes behind its distribution or its sensitivity to future anthropogenic pressures.

Despite an unprecedented sampling effort, vent fauna diversity in the Southwest Pacific region remains underestimated (only 116 taxa identified). Nevertheless, our study provides unique insights into the diversity of the study area and makes a significant contribution to advancing scientific knowledge. A previous study identified 159 taxa across the Southwest Pacific region, including the Manus, North Fiji and Lau basins, and the Feni Tabar, Vanutatu (New Hebrides), Tonga-Tofua and Kermadec Arcs, or 143 taxa excluding the Kermadec arc further south in the region (see Table 2 in Appendix S1 in Tunnicliffe et al., 2024). That study considered macrofaunal species from all habitats influenced by hydrothermal fluids, thereby encompassing a broader range of habitats than ours. Despite these differences, it is noteworthy that we identified 32 new taxa at the genus or species level (see taxa highlighted in bold in Appendix D) that were absent from their list. Focusing on the three basin the two studies have in common; we identified 25 new taxa at the genus or species level for the Manus Basin, 22 for the Lau Basin and 10 for the North Fiji Basin. Our study also provides the first detailed characterization description of the Woodlark Basin hydrothermal fauna, a region not covered by Tunnicliffe et al. (2024), thereby enhancing and updating the work of Boulart et al. (2022).

4.2. The habitat effect on community structure

Over a third of identified taxa are common to all three habitats (40 %), suggesting many species may tolerate a wide range of vent conditions. Small macrofauna are not exclusive to specific megafaunal habitats but rather to local microhabitats present in different assemblages, as observed on the EPR (Mills et al., 2007; Matabos et al., 2008). This aligns with the observed spatial organization of holobiont patches which strongly overlap within a sampling area, accounting for variable proportions of each engineer species in the samples. Habitat organization occurred both horizontally and vertically, with *Ifremeria* individuals found beneath *Alviniconcha* specimens, creating transition zones that likely account for their many shared species. The *Bathymodiolus* habitat was more spatially isolated and comprised the highest number of exclusive species, about a quarter of the identified taxa. These taxa mainly belong to genera or families also associated with the sessile barnacle *E. ohtai*, found at the periphery where temperature values are close to ambient seawater (Collins et al., 2012), suggesting temperature as a limiting factor in their distribution. This included *Actinaria* cnidarians, *Chiridota* or Ophiuroidae echinoderms, *Munidopsis* squat lobsters, *Phymorhynchus* gastropods, *Ophryotrocha* dorvilleids and *Nicomache* maldanids, also abundant in the stalked cirriped *Vulcanolepas* thickets in the Woodlark Ridge (Boulart et al., 2022). In contrast, the *Ifremeria* or *Alviniconcha* habitat has fewer exclusive species, with rarity

rather than habitat likely explaining this exclusivity.

The three engineer species by providing both habitat and food, increase the number of local ecological niches for smaller mobile macrofaunal species and contribute to enhance local diversity (e.g., Govenar et al., 2005). Species richness was lower in the *Alviniconcha* habitat compared to the *Ifremeria* and *Bathymodiolus* habitats. In situ videos recorded during the expedition using autonomous camera systems over several days, showed that *Alviniconcha* gastropods are more mobile than *Ifremeria* gastropods and *Bathymodiolus* mussels (M. Matabos, unpublished data), probably in response to bursts of temperatures. This aligns with S(VI)/Mn ratios and the % Endmember fluid, indicating that *Alviniconcha* are found in areas more impacted by hydrothermal fluids, subject to greater physico-chemical fluctuations than *Bathymodiolus*. Higher mobility might allow them to reposition themselves to escape harmful conditions as observed for the large mussels of *Bathymodiolus azoricus* (Van Audenhaege et al., 2022) but could prevent the creation of stable ecological niches available for smaller macrofauna and may explain the lower diversity observed. Additionally, the lower diversity might result from species physiological tolerance to harsher, more variable conditions, characteristic of this habitat, or their nutritional specificities (especially for symbiotic species). Temperature, sulfide concentrations, geological and biological controls were all suggested to contribute to the Lau Basin megafauna zonation (Desbruyères et al., 1994; Henry et al., 2008; Podowski et al., 2009; Kim and Hammerstrom, 2012; Diaz-Recio Lorenzo et al., 2021). Our large dataset of environmental variables reflects the strong environmental heterogeneity that can be found in *Ifremeria* and *Alviniconcha* habitats that contrasts with the more homogeneous conditions measured in the *Bathymodiolus* habitat. Interestingly, the few taxa common to these first two habitats were either mobile polychaetes (e.g., Polynoids Lepidonotopodini) or species known to tolerate, or at least, belong to a genus known to tolerate, high H_2S concentrations or temperatures (i.e., *A. boucheti* or genus *Paralvinella*) (Desbruyères and Laubier, 1989; Beinart et al., 2012; Hourdez and Jollivet, 2020).

Although richness effects are an important part of the diversity variation between *Bathymodiolus* and *Alviniconcha* habitats, the main factor driving diversity changes along the three habitats in the Lau Basin was species replacement, which may result from environmental filtering along the local diffuse flow environmental gradient (Alfaro-Lucas et al., 2020). Species distribute along the gradient resulting from the mixing between vent fluid and seawater according to environmental conditions, leading to a high β-diversity as species are replaced by others. While species replacement dominates between *Ifremeria* and *Bathymodiolus* habitats in the Manus Basin, richness difference is the dominant component of the observed β-diversity between the *Alviniconcha* habitat and the two other habitats. While our taxonomic resolution may minimize the proportion of species replacement, its effect is unlikely to be major here, given that most cases of cryptic species are linked to geography. More likely, the harsher environmental conditions existing in this habitat could enhance the nestedness in which only a subset of species are better adapted to cope with the local environmental conditions.

Despite this insight, the environment explains a relatively low proportion of the variance between assemblages. The variables considered in this study may not be sufficient to properly characterize the environment, or our methodological approach may have failed to properly measure conditions experienced by organisms. For instance, our chemical measurements protocol might not fully capture local spatial heterogeneity and temporal variability. At vents, conditions are highly variable at the centimeter scale, necessitating multiple temporal and spatial measurements for a proper characterization (Le Bris et al., 2005; Lee et al., 2015; Van Audenhaege et al., 2022). The 3D structure of the habitat created by the shells or the tubes of megafauna can also generate local environmental gradients, as observed within the *Alvinella pompejana* habitat (Le Bris et al., 2005). Hence, some small megafauna or meiofauna observed in the habitat may occupy specific micro-habitats that differ from the general surrounding chemistry described in this study. In addition to the horizontal and vertical environmental heterogeneity, small-scale temporal fluctuation adds to environmental heterogeneity on scales from seconds to hours (Johnson et al., 1988; Lee et al., 2015; Van Audenhaege et al., 2022), as illustrated by the temperature ranges recorded in this study. This small-scale spatiotemporal variability could strongly impact species distributions, depending on their ability to cope with a wide range of conditions (Bates et al., 2010). It is also worth noting that our measurements do not consider the chemical consumption by biological fauna to sustain their own biomass through chemoautotrophic symbiosis. Although this process might be neglectable when considering the fluid brought by mixing and turbulence from nearby focused exits (see Marcon et al., 2013 for *Bathymodiolus* along the Mid-Atlantic Ridge), concentrations of CH_4 and sulfur measured above the assemblage might not be fully representative of the fluid diffusing beneath the organisms at very local scales.

4.3. Biogeography

Our presence-absence analysis of the communities' composition highlights a split between the western (Manus/Woodlark) and eastern (North Fiji/Lau/Futuna) regions. Previous studies already reported such a biogeographical break, both at the population and species levels. Geographic divergence between populations from the Manus Basin and the North Fiji/Lau basins occurs within various phyla, including gastropods like the snails *Ifremeria nautilei* and *Alviniconcha kojimai* (Thaler et al., 2011; Tran Lu Y et al., 2022, 2025) and *Provanna* (Poitrimol et al., 2022), limpets such as *Symmetromphalus*, *Lepetodrilus* and *Shinkailepas,* the bivalve *Bathymodiolus manusensis,* the polychaete *Branchipolynoe segonzaci* (ex. *Branchinotogluma segonzaci),* (Plouviez et al., 2019; Poitrimol et al., 2022; Tran Lu Y et al., 2025), and crustaceans like the shrimp *Rimicaris* spp. (Thaler et al., 2014), the crabs *Austinograea* (Lee et al., 2019), the stalked barnacles *Vulcanolepas* (Chan and Chang, 2018; Chan et al., 2019; Boulart et al., 2022) or the cirriped *Eochionelasmus ohtai* (Tran Lu Y et al., 2025). Our study confirmed a geographic split in community diversity and composition, with species replacement as the main driver of biodiversity changes along the longitudinal gradient, mainly in the *Bathymodiolus* and *Ifremeria* habitats. This could be explained by the occurrence of species restricted to either the Eastern or the Western basins (e.g., the polynoids *Branchipolynoe* aff. *marianus* A from the East vs. *B.* aff. *marianus B* from the West or *B.* aff. *trifurcus* and *B. trifurcus*). We expect that this effect would become more visible in the *Alviniconcha* habitat with a greater taxonomic resolution.

Tectonic history and ocean circulation are key factors explaining the biogeographic patterns of hydrothermal vent fauna along mid-ocean ridges (Tunnicliffe, 1991; Van Dover, 2002; Plouviez et al., 2009; Matabos et al., 2011; Matabos and Jollivet, 2019; Watanabe et al., 2019). In Southwest Pacific, the New Guinea archipelago isolates the Manus Basin, forming a physical barrier that limits exchanges with other basins (Thaler et al., 2011) and can account for its high endemism. Similarly, several species were only found in the eastern basins (e.g., *Bruceiella globulus*, *Symmetriapelta* spp., *Branchipolynoe trifurcus* and *B.* aff. *marianus* A). The barrier efficiency will depend on species life-history traits, such as larval dispersal, behaviour and life span, with connectivity between the Eastern and Western basins being limited for species with short planktonic larval duration (Mitarai et al., 2016; Poitrimol et al., 2022; Diaz-Recio Lorenzo et al., 2023). Phylogeographic patterns can strongly vary among taxa, with some species connecting across the full geographical gradient while others are more localized (Poitrimol et al., 2022; Diaz-Recio Lorenzo et al., 2023). The influence of the Northwest Pacific on the species composition of the Manus Basin with possible connections more specific to this basin, as illustrated by the presence of *Provanna clathrata* or *Desbruyeresia costata* in our dataset (both described from the Okinawa Trough), may contribute to the observed divide. Alternatively, the split observed may also reflect a data gap and insufficient sampling in the Vanuatu and Solomon regions, which may have an important role connecting Eastern and Western basins (Mitarai et al.,

2016). Further sampling is needed in intermediate sites to test for the occurrence of a continuum in faunal composition along the Southwest Pacific. The presence of 'phantom sites' have already been suggested along the mid-Atlantic ridge to account for connectivity observed over large distances (Breusing et al., 2016). Hydrothermal vents are dynamic environments with sites or fields becoming inactive or reactivated, as observed during the CHUBACARC cruise (S. Hourdez, personal observation, 2019), and new sites being regularly discovered in the region (e.g., Boulart et al., 2022), resulting in a constantly evolving distribution of active sites.

Interestingly, faunal assemblages in the Woodlark Basin, although under-represented by a few samples, differed from all other locations. Assemblages from La Scala vent field included some endemic limpet species (*Shinkailepas* aff. *tufari* Woodlark, *Symmetromphalus mithril* and *Symmetriapelta radiata*), species widely distributed across basins (e.g., *Thermopolynoe branchiata* polynoids, *Rimicaris variabilis* shrimp), or others only shared with the Manus basins assemblages (e.g., *Paralvinella hessleri*, *Branchinpolynoe* aff. *marianus* B) and represents a multi-species hybrid zone for some species (*Lepetodrilus fijiensis/L. schrolli* or *Shinkailepas tollmanni/aff. tollmanni*) (Tran Lu Y et al., 2025). Woodlark was the deepest basin visited during the CHUBACARC cruise, La Scala vent site being located at 3388 m depth against 2716 m for the next deepest site located in the Lau Basin (i.e., Tow Cam). While depth could be an important factor in structuring biodiversity and species distribution as suggested in our multivariate analyses (Desbruyères et al., 2001; Watanabe et al., 2019), the Woodlark Basin particularity is more likely to reside in its intermediate geographical position between the Manus Basin and the eastern region, supporting its role as a biological stepping-stone, as previously suggested by Boulart et al. (2022) and Poitrimol et al. (2022).

4.4. Implication for biodiversity conservation

Patterns of diversity and variation provide critical information to inform relevant environmental management and conservation strategies (Gering et al., 2003; Clough et al., 2007; Socolar et al., 2016; Carlos-Júnior et al., 2019). Depending on the drivers of diversity variation within communities – either species replacement or differences in species richness - the appropriate conservation measures may differ (Socolar et al., 2016). For example, areas with diversity driven by species turnover may require strategies focused on maintaining connectivity between sites to facilitate species migration and ensure ecosystem resilience, requiring protection of multiple areas. In contrast, areas with high richness difference may benefit more from conservation efforts aimed at protecting specific sites or habitats critical for supporting diverse species assemblages (Socolar et al., 2016). If species replacement dominates diversity variation at the regional scale for at least mussel beds and *Ifremeria* clumps, richness difference remains an important process in the Manus Basin. Consequently, Eastern and Western basins, both potentially subject to anthropogenic disturbance if the mining moratorium is not extended, may require different management plans to conserve biodiversity.

Species replacement primarily drives diversity variation in the Southwest Pacific vents, reflecting the restricted geographical range of certain species. Because of a high rate of geographic species crypticism, we expect this process to be even more pronounced with greater taxonomic resolution. This emphasizes the importance of enhancing taxonomic efforts in this region and identifying specific diagnostic morphological traits between cryptic species already evidenced by the molecular barcode. Key areas that may act as transition zones between eastern and western biogeographic entities, or those that exhibit higher endemism, should be prioritized for biodiversity conservation. The Woodlark Basin, where endemism was likely underestimated, might be crucial for connecting the Manus Basin and the eastern Fiji/Lau/Futuna sub-region, and could represent a larval recipient for Manus communities. Additionally, the Manus Basin, characterized by its central geographical position and its strong tectonic activity is also likely to act as a transition zone between the North and Southwest Pacific (Tunnicliffe et al., 2024) with a greater species diversification. This should therefore represent a major concern for the vent diversity conservation.

Habitat availability is also essential to community resilience as it influences recruitment success and the replenishment of local populations at the metapopulation scale (Mullineaux et al., 2018). A significant loss of habitat in the Woodlark Basin could critically affect connectivity between the Manus Basin and other eastern basins. In addition, because mussel beds where not found at the La Scala site and rare along the North Fiji ridge and Futuna Volcanic Arc despite a great larval dispersal potential of the mussels, species associated with this habitat may have more difficulties to expand at large scales, and therefore may be less resilient to disturbance. Furthermore, as the *Bathymodiolus* habitat supports a significant proportion of the regional biodiversity, a major loss of these mussel beds in the Manus and Lau basins could have a major impact on Southwestern Pacific biodiversity. Devastating geological events are probably more common in the region than previously thought, with obvious implications for recolonization dynamics (Beinart et al., 2024). Significant mussel population losses were observed following the eruption of the Hunga submarine volcano in 2022, more than two years after the CHUBACARC expedition (Beinart et al., 2024). Two fields along the ridge, Tow Cam and ABE, which were sampled as part of our study, experienced notable declines, particularly Tow Cam, located closest to the volcano. In contrast, mussel communities in the Tui Malila field, situated further south, were unaffected by the eruption and could contribute to the recolonization of impacted sites further north. Monitoring efforts established in this region, coupled with data from our study as a baseline, will enable the evaluation of community resilience after a major disturbance and provide valuable insights to inform environmental management strategies.

CRediT authorship contribution statement

Camille Poitrimol: Writing – review & editing, Writing – original draft, Visualization, Validation, Supervision, Software, Methodology, Investigation, Formal analysis, Data curation, Conceptualization. **Éric Thiébaut:** Writing – review & editing, Writing – original draft, Validation, Supervision, Resources, Project administration, Methodology, Investigation, Funding acquisition, Formal analysis, Conceptualization. **Cédric Boulart:** Writing – review & editing, Validation, Resources, Investigation, Data curation, Conceptualization. **Cécile Cathalot:** Writing – review & editing, Validation, Resources, Investigation, Data curation, Conceptualization. **Olivier Rouxel:** Writing – review & editing, Resources, Conceptualization, Investigation. **Didier Jollivet:** Writing – review & editing, Resources, Investigation, Funding acquisition, Conceptualization. **Stéphane Hourdez:** Writing – review & editing, Validation, Resources, Investigation, Funding acquisition, Data curation, Conceptualization. **Marjolaine Matabos:** Writing – review & editing, Writing – original draft, Validation, Supervision, Resources, Project administration, Methodology, Investigation, Funding acquisition, Formal analysis, Data curation, Conceptualization.

Funding

Agence Nationale pour la Recherche (ANR): project CERBERUS (contract number ANR-17-CE02- 0003; https://anr.fr/); Ifremer; French Oceanographic Fleet.

Declaration of competing interest

The authors declare that they have no known competing financial interests or personal relationships that could have appeared to influence the work reported in this paper.

Acknowledgments

We thank the captain and crew of the RV *L'Atalante* and the ROV *Victor 6000* team for their work at sea. We also thank the entire CHUBACARC scientific team, especially T. Comtet, T. Broquet, S. L'Haridon, L. Michel and V. Le Layec for their support in sorting samples on board, as well as E. Rinnert, A. Boissier and N. Gayet for their help in deploying in situ PIF and CHEMINI instruments and recovering and processing fluid samples on board. We are grateful to A. Laes for lending us the CHEMINI instrument. We thank E.-J. Pernet and M. Le Pans for their assistance in sorting samples at the Brest Ifremer deep-sea laboratory. Thanks to J. Castel, V. Cueff-Gauchard, A. Tran Lu Y, and A. Chabert for sharing barcoding data produced as part of the ANR Cerberus project, and to all those involved in producing this dataset: C. Daguin-Thiébaut, A.-S. Le Port, M. Ballenghien, S. Ruault, S. Arnaud-Haond, F. Bonhomme and P.-A. Gagnaire. We also thank C. Chen for confirming some gastropod species identifications and A.-S. Alix for the maps included in Appendix. We are also grateful to the two anonymous reviewers for their comments and suggestions, which have contributed to the improvement of our paper. This work was supported by the Agence Nationale pour la Recherche (ANR): project CERBERUS (contract number ANR-17-CE02-0003; https://anr.fr/). CP was funded by Ph.D grants from the ANR CERBERUS and Ifremer. Participation to the research cruise also benefitted from the French Oceanographic Fleet.

Appendix A - E. Supplementary data

Supplementary data to this article can be found online at https://doi.org/10.1016/j.scitotenv.2025.178694.

Data availability

Datasets generated for this study are in the Appendix. Taxa per sample data are in the SEANOE database: https://doi.org/10.17882/102270. Further inquiries can be directed to the corresponding author.

References

Alfaro-Lucas, J.M., Pradillon, F., Zeppilli, D., Michel, L.N., Martinez-Arbizu, P., Tanaka, H., et al., 2020. High environmental stress and productivity increase functional diversity along a deep-sea hydrothermal vent gradient. Ecology 101, e03144. https://doi.org/10.1002/ecy.3144.

Anderson, M.J., Crist, T.O., Chase, J.M., Vellend, M., Inouye, B.D., Freestone, A.L., et al., 2011. Navigating the multiple meanings of β diversity: a roadmap for the practicing ecologist. Ecol. Lett. 14, 19–28. https://doi.org/10.1111/j.1461-0248.2010.01552.x.

Bates, A.E., Tunnicliffe, V., Lee, R.W., 2005. Role of thermal conditions in habitat selection by hydrothermal vent gastropods. Mar. Ecol. Prog. Ser. 305, 1–15. https://doi.org/10.3354/meps305001.

Bates, A.E., Lee, R.W., Tunnicliffe, V., Lamare, M.D., 2010. Deep-sea hydrothermal vent animals seek cool fluids in a highly variable thermal environment. Nat. Commun. 1, 14. https://doi.org/10.1038/ncomms1014.

Beaulieu, S.E., Baker, E.T., German, C.R., Maffei, A., 2013. An authoritative global database for active submarine hydrothermal vent fields. Geochem. Geophys. Geosystems 14, 4892–4905. https://doi.org/10.1002/2013GC004998.

Beinart, R.A., Sanders, J.G., Faure, B., Sylva, S.P., Lee, R.W., Becker, E.L., et al., 2012. Evidence for the role of endosymbionts in regional-scale habitat partitioning by hydrothermal vent symbioses. Proc. Natl. Acad. Sci. 109, E3241–E3250. https://doi.org/10.1073/pnas.1202690109.

Beinart, R.A., Arellano, S.M., Chaknova, M., Meagher, J., Davies, A.J., Lopresti, J., et al., 2024. Deep seafloor hydrothermal vent communities buried by volcanic ash from the 2022 Hunga eruption. Commun. Earth Environ. 5, 1–10. https://doi.org/10.1038/s43247-024-01411-w.

Bézos, A., Escrig, S., Langmuir, C.H., Michael, P.J., Asimow, P.D., 2009. Origins of chemical diversity of back-arc basin basalts: a segment-scale study of the Eastern Lau Spreading Center. J. Geophys. Res. Solid Earth 114. https://doi.org/10.1029/2008JB005924.

Boschen, R.E., Rowden, A.A., Clark, M.R., Gardner, J.P.A., 2013. Mining of deep-sea seafloor massive sulfides: a review of the deposits, their benthic communities, impacts from mining, regulatory frameworks and management strategies. Ocean Coast. Manag. 84, 54–67. https://doi.org/10.1016/j.ocecoaman.2013.07.005.

Boschen-Rose, R.E., Clark, M.R., Rowden, A.A., Gardner, J.P.A., 2021. Assessing the ecological risk to deep-sea megafaunal assemblages from seafloor massive sulfide mining using a functional traits sensitivity approach. Ocean Coast. Manag. 210, 105656. https://doi.org/10.1016/j.ocecoaman.2021.105656.

Boulart, C., Rouxel, O., Scalabrin, C., Le Meur, P., Pelleter, E., Poitrimol, C., et al., 2022. Active hydrothermal vents in the Woodlark Basin may act as dispersing centres for hydrothermal fauna. Commun. Earth Environ. 3, 1–16. https://doi.org/10.1038/s43247-022-00387-9.

Breusing, C., Biastoch, A., Drews, A., Metaxas, A., Jollivet, D., Vrijenhoek, R.C., et al., 2016. Biophysical and population genetic models predict the presence of "Phantom" stepping stones connecting Mid-Atlantic Ridge vent ecosystems. Curr. Biol. 26, 2257–2267. https://doi.org/10.1016/j.cub.2016.06.062.

Carlos-Júnior, L.A., Spencer, M., Neves, D.M., Moulton, T.P., Pires, D. de O., e Castro, C. B., et al., 2019. Rarity and beta diversity assessment as tools for guiding conservation strategies in marine tropical subtidal communities. Divers. Distrib. 25, 743–757. https://doi.org/10.1111/ddi.12896.

Castel, J., Hourdez, S., Pradillon, F., Daguin-Thiébaut, C., Ballenghien, M., Ruault, S., et al., 2022. Inter-specific genetic exchange despite strong divergence in deep-sea hydrothermal vent gastropods of the genus *Alviniconcha*. Genes 13, 985. https://doi.org/10.3390/genes13060985.

Chan, B.K.K., Chang, Y.-W., 2018. A new deep-sea scalpelliform barnacle, *Vulcanolepas buckeridgei* sp. nov. (Eolepadidae: Neolepadinae) from hydrothermal vents in the Lau Basin. Zootaxa 4407, 117. https://doi.org/10.11646/zootaxa.4407.1.8.

Chan, B.K.K., Ju, S.-J., Kim, S.-J., 2019. A new species of hydrothermal vent stalked barnacle *Vulcanolepas* (Scalpelliforms: Eolepadidae) from the North Fiji Basin, Southwestern Pacific Ocean. Zootaxa 4563, 135–148.

Chase, J.M., Myers, J.A., 2011. Disentangling the importance of ecological niches from stochastic processes across scales. Philos. Trans. R. Soc. B Biol. Sci. 366, 2351–2363. https://doi.org/10.1098/rstb.2011.0063.

Chen, C., Sigwart, J.D., 2023. The lost vent gastropod species of Lothar A. Beck. Zootaxa 5270, 401–436. https://doi.org/10.11646/zootaxa.5270.3.2.

Chen, C., Watanabe, H.K., 2020. Substrate-dependent shell morphology in a deep-sea vetigastropod limpet. Mar. Biodivers. 50, 104. https://doi.org/10.1007/s12526-020-01135-y.

Chen, C., Watanabe, H.K., Nagai, Y., Toyofuku, T., Xu, T., Sun, J., et al., 2019. Complex factors shape phenotypic variation in deep-sea limpets. Biol. Lett. 15, 20190504. https://doi.org/10.1098/rsbl.2019.0504.

Chen, C., Poitrimol, C., Matabos, M., 2024. Integrative taxonomy of new neomphaloidean gastropods from deep-sea hot vents of the southwestern Pacific. Zool. J. Linn. Soc. https://doi.org/10.1093/zoolinnean/zlae064.

Chevaldonné, P., Godfroy, A., 1997. Enumeration of microorganisms from deep-sea hydrothermal chimney samples. FEMS Microbiol. Lett. 146, 211–216. https://doi.org/10.1111/j.1574-6968.1997.tb10195.x.

Clough, Y., Holzschuh, A., Gabriel, D., Purtauf, T., Kleijn, D., Kruess, A., et al., 2007. Alpha and beta diversity of arthropods and plants in organically and conventionally managed wheat fields. J. Appl. Ecol. 44, 804–812. https://doi.org/10.1111/j.1365-2664.2007.01294.x.

Collins, P.C., Kennedy, R., Van Dover, C.L., 2012. A biological survey method applied to seafloor massive sulphides (SMS) with contagiously distributed hydrothermal-vent fauna. Mar. Ecol. Prog. Ser. 452, 89–107. https://doi.org/10.3354/meps09646.

Cotte, L., Waeles, M., Pernet-Coudrier, B., Sarradin, P.-M., Cathalot, C., Riso, R.D., 2015. A comparison of in situ vs. ex situ filtration methods on the assessment of dissolved and particulate metals at hydrothermal vents. Deep Sea Res. Part Oceanogr. Res. Pap. 105, 186–194. https://doi.org/10.1016/j.dsr.2015.09.005.

Desbruyères, D., Laubier, L., 1989. *Paralvinella hessleri*, new species of Alvinellidae (Polychaeta) from the Mariana Back-Arc Basin hydrothermal vents. Proc. Biol. Soc. Wash. 102, 761–767.

Desbruyères, D., Alayse-Danet, A.-M., Ohta, S., the Scientific Parties of biolauand starmerCruises, 1994. Deep-sea hydrothermal communities in Southwestern Pacific back-arc basins (the North Fiji and Lau Basins): composition, microdistribution and food web. Mar. Geol. 116, 227–242. https://doi.org/10.1016/0025-3227(94)90178-3.

Desbruyères, D., Biscoito, M., Caprais, J.-C., Colaço, A., Comtet, T., Crassous, P., et al., 2001. Variations in deep-sea hydrothermal vent communities on the Mid-Atlantic Ridge near the Azores plateau. Deep Sea Res. Part Oceanogr. Res. Pap. 48, 1325–1346. https://doi.org/10.1016/S0967-0637(00)00083-2.

Desbruyères, D., Hashimoto, J., Fabri, M.-C., 2006a. Composition and biogeography of hydrothermal vent communities in Western Pacific Back-Arc Basins. In: Christie, D. M., Fisher, C.R., Lee, S.-M., Givens, S. (Eds.), Geophysical Monograph Series. American Geophysical Union, Washington D. C, pp. 215–234.

Desbruyères, D., Segonzac, M., Bright, M., 2006b. Handbook of Deep-sea Hydrothermal vent fauna., Second Edition. Denisia 18.

Diaz-Recio Lorenzo, C., ter Bruggen, D., Luther, G.W., Gartman, A., Gollner, S., 2021. Copepod assemblages along a hydrothermal stress gradient at diffuse flow habitats within the ABE vent site (Eastern Lau Spreading Center, Southwest Pacific). Deep Sea Res. Part Oceanogr. Res. Pap. 173, 103532. https://doi.org/10.1016/j.dsr.2021.103532.

Diaz-Recio Lorenzo, C., Patel, T., Arsenault-Pernet, E.-J., Poitrimol, C., Jollivet, D., Martinez Arbizu, P., et al., 2023. Highly structured populations of deep-sea copepods associated with hydrothermal vents across the Southwest Pacific, despite contrasting life history traits. PloS One 18, e0292525. https://doi.org/10.1371/journal.pone.0292525.

Dick, G.J., 2019. The microbiomes of deep-sea hydrothermal vents: distributed globally, shaped locally. Nat. Rev. Microbiol. 17, 271–283. https://doi.org/10.1038/s41579-019-0160-2.

Donval, J.-P., Charlou, J.-L., Lucas, L., 2008. Analysis of light hydrocarbons in marine sediments by headspace technique: optimization using design of experiments.

Chemom. Intel. Lab. Syst. 94, 89–94. https://doi.org/10.1016/j.chemolab.2008.06.010.
Dray, S., Bauman, D., Blanchet, G., Borcard, D., Clappe, S., Guenard, G., et al., 2022. adespatial: multivariate multiscale spatial analysis. Available at: https://CRAN.R-project.org/package=adespatial. (Accessed 7 June 2022).
Evans, G.N., Tivey, M.K., Monteleone, B., Shimizu, N., Seewald, J.S., Rouxel, O.J., 2020. Trace element proxies of seafloor hydrothermal fluids based on secondary ion mass spectrometry (SIMS) of black smoker chimney linings. Geochim. Cosmochim. Acta 269, 346–375. https://doi.org/10.1016/j.gca.2019.09.038.
Fouquet, Y., Pelleter, E., Konn, C., Chazot, G., Dupré, S., Alix, A.S., et al., 2018. Volcanic and hydrothermal processes in submarine calderas: the Kulo Lasi example (SW Pacific). Ore Geol. Rev. 99, 314–343. https://doi.org/10.1016/j.oregeorev.2018.06.006.
Galkin, S.V., 1997. Megafauna associated with hydrothermal vents in the Manus Back-Arc Basin (Bismarck Sea). Mar. Geol. 142, 197–206. https://doi.org/10.1016/S0025-3227(97)00051-0.
Gering, J.C., Crist, T.O., Veech, J.A., 2003. Additive partitioning of species diversity across multiple spatial scales: implications for regional conservation of biodiversity. Conserv. Biol. 17, 488–499. https://doi.org/10.1046/j.1523-1739.2003.01465.x.
Giguère, T.N., Tunnicliffe, V., 2021. Beta diversity differs among hydrothermal vent systems: implications for conservation. PloS One 16, e0256637. https://doi.org/10.1371/journal.pone.0256637.
Gollner, S., Kaiser, S., Menzel, L., Jones, D.O.B., Brown, A., Mestre, N.C., et al., 2017. Resilience of benthic deep-sea fauna to mining activities. Mar. Environ. Res. 129, 76–101. https://doi.org/10.1016/j.marenvres.2017.04.010.
Govenar, B., Le Bris, N., Gollner, S., Glanville, J., Aperghis, A.B., Hourdez, S., et al., 2005. Epifaunal community structure associated with *Riftia pachyptila* aggregations in chemically different hydrothermal vent habitats. Mar. Ecol. Prog. Ser. 305, 67–77. https://doi.org/10.3354/meps305067.
Gray, J.S., 2000. The measurement of marine species diversity, with an application to the benthic fauna of the Norwegian continental shelf. J. Exp. Mar. Biol. Ecol. 250, 23–49. https://doi.org/10.1016/S0022-0981(00)00178-7.
Hall, R., 2002. Cenozoic geological and plate tectonic evolution of SE Asia and the SW Pacific: computer-based reconstructions, model and animations. J. Asian Earth Sci. 20, 353–431. https://doi.org/10.1016/S1367-9120(01)00069-4.
Henry, M.S., Childress, J.J., Figueroa, D., 2008. Metabolic rates and thermal tolerances of chemoautotrophic symbioses from Lau Basin hydrothermal vents and their implications for species distributions. Deep Sea Res. Part Oceanogr. Res. Pap. 55, 679–695. https://doi.org/10.1016/j.dsr.2008.02.001.
Herzig, P.M., Hannington, M.D., Fouquet, Y., von Stackelberg, U., Petersen, S., 1993. Gold-rich polymetallic sulfides from the Lau back arc and implications for the geochemistry of gold in sea-floor hydrothermal systems of the Southwest Pacific. Econ. Geol. 88, 2182–2209. https://doi.org/10.2113/gsecongeo.88.8.2182.
Hoagland, P., Beaulieu, S., Tivey, M.A., Eggert, R.G., German, C., Glowka, L., et al., 2010. Deep-sea mining of seafloor massive sulfides. Mar. Policy 34, 728–732. https://doi.org/10.1016/j.marpol.2009.12.001.
Hourdez, S., Jollivet, D., 2019. CHUBACARC cruise, L'Atalante R/V. https://doi.org/10.17600/18001111.
Hourdez, S., Jollivet, D., 2020. Metazoan adaptation to deep-sea hydrothermal vents. In: di Prisco, G., Edwards, H.G.M., Elster, J., Huiskes, A.H.L. (Eds.), Life in Extreme Environments: Insights in Biological Capability. Cambridge University Press, pp. 42–67.
James, R.H., Green, D.R.H., Stock, M.J., Alker, B.J., Banerjee, N.R., Cole, C., et al., 2014. Composition of hydrothermal fluids and mineralogy of associated chimney material on the East Scotia Ridge back-arc spreading centre. Geochim. Cosmochim. Acta 139, 47–71. https://doi.org/10.1016/j.gca.2014.04.024.
Jamieson, J.W., Gartman, A., 2020. Defining active, inactive, and extinct seafloor massive sulfide deposits. Mar. Policy 117, 103926. https://doi.org/10.1016/j.marpol.2020.103926.
Johnson, K.S., Childress, J.J., Beehler, C.L., 1988. Short-term temperature variability in the Rose Garden hydrothermal vent field: an unstable deep-sea environment. Deep Sea Res. Part Oceanogr. Res. Pap. 35, 1711–1721. https://doi.org/10.1016/0198-0149(88)90045-3.
Josso, P., Pelleter, E., Pourret, O., Fouquet, Y., Etoubleau, J., Cheron, S., et al., 2017. A new discrimination scheme for oceanic ferromanganese deposits using high field strength and rare earth elements. Ore Geol. Rev. 87, 3–15. https://doi.org/10.1016/j.oregeorev.2016.09.003.
Kakee, T., 2020. Deep-sea mining legislation in Pacific Island countries: from the perspective of public participation in approval procedures. Mar. Policy 103881. https://doi.org/10.1016/j.marpol.2020.103881.
Kim, S., Hammerstrom, K., 2012. Hydrothermal vent community zonation along environmental gradients at the Lau back-arc spreading center. Deep Sea Res. Part Oceanogr. Res. Pap. 62, 10–19. https://doi.org/10.1016/j.dsr.2011.12.010.
Klinkhammer, G., Hudson, A., 1986. Dispersal patterns for hydrothermal plumes in the South Pacific using manganese as a tracer. Earth Planet. Sci. Lett. 79, 241–249. https://doi.org/10.1016/0012-821X(86)90182-2.
Klinkhammer, G., Bender, M., Weiss, R.F., 1977. Hydrothermal manganese in the Galapagos Rift. Nature 269, 319–320. https://doi.org/10.1038/269319a0.
Konn, C., Fourré, E., Jean-Baptiste, P., Donval, J.P., Guyader, V., Birot, D., et al., 2016. Extensive hydrothermal activity revealed by multi-tracer survey in the Wallis and Futuna region (SW Pacific). Deep Sea Res. Part Oceanogr. Res. Pap. 116, 127–144. https://doi.org/10.1016/j.dsr.2016.07.012.
Le Bris, N., Sarradin, P.-M., Caprais, J.-C., 2003. Contrasted sulphide chemistries in the environment of 13°N EPR vent fauna. Deep Sea Res. Part Oceanogr. Res. Pap. 50, 737–747. https://doi.org/10.1016/S0967-0637(03)00051-7.
Le Bris, N., Zbinden, M., Gaill, F., 2005. Processes controlling the physico-chemical micro-environments associated with Pompeii worms. Deep Sea Res. Part Oceanogr. Res. Pap. 52, 1071–1083. https://doi.org/10.1016/j.dsr.2005.01.003.
Lee, R.W., Robert, K., Matabos, M., Bates, A.E., Juniper, S.K., 2015. Temporal and spatial variation in temperature experienced by macrofauna at Main Endeavour hydrothermal vent field. Deep Sea Res. Part Oceanogr. Res. Pap. 106, 154–166. https://doi.org/10.1016/j.dsr.2015.10.004.
Lee, W.-K., Kim, S.-J., Hou, B.K., Van Dover, C.L., Ju, S.-J., 2019. Population genetic differentiation of the hydrothermal vent crab *Austinograea alayseae* (Crustacea: Bythograeidae) in the Southwest Pacific Ocean. PloS One 14, e0215829. https://doi.org/10.1371/journal.pone.0215829.
Legendre, P., 2014. Interpreting the replacement and richness difference components of beta diversity. Glob. Ecol. Biogeogr. 23, 1324–1334. https://doi.org/10.1111/geb.12207.
Legendre, P., Anderson, M.J., 1999. Distance-based redundancy analysis: testing multispecies responses in multifactorial ecological experiments. Ecological monographs 69, 1–24. https://doi.org/10.1890/0012-9615(1999)069[0001:DBRATM]2.0.CO;2.
Leibold, M.A., Holyoak, M., Mouquet, N., Amarasekare, P., Chase, J.M., Hoopes, M.F., et al., 2004. The metacommunity concept: a framework for multi-scale community ecology. Ecol. Lett. 7, 601–613. https://doi.org/10.1111/j.1461-0248.2004.00608.x.
Leprieur, F., Tedesco, P.A., Hugueny, B., Beauchard, O., Dürr, H.H., Brosse, S., et al., 2011. Partitioning global patterns of freshwater fish beta diversity reveals contrasting signatures of past climate changes. Ecol. Lett. 14, 325–334. https://doi.org/10.1111/j.1461-0248.2011.01589.x.
Levesque, C., Juniper, S.K., Marcus, J., 2003. Food resource partitioning and competition among alvinellid polychaetes of Juan de Fuca Ridge hydrothermal vents. Mar. Ecol. Prog. Ser. 246, 173–182. https://doi.org/10.3354/meps246173.
Luther, G.W., Rozan, T.F., Taillefert, M., Nuzzio, D.B., Di Meo, C., Shank, T.M., et al., 2001. Chemical speciation drives hydrothermal vent ecology. Nature 410, 813–816. https://doi.org/10.1038/35071069.
Marcon, Y., Sahling, H., Borowski, C., dos Santos Ferreira, C., Thal, J., Bohrmann, G., 2013. Megafaunal distribution and assessment of total methane and sulfide consumption by mussel beds at Menez Gwen hydrothermal vent, based on geo-referenced photomosaics. Deep Sea Res. I 75, 93–109. https://doi.org/10.1016/j.dsr.2013.01.008.
Matabos, M., Jollivet, D., 2019. Revisiting the Lepetodrilus elevatus species complex (Vetigastropoda: Lepetodrilidae), using samples from the Galápagos and Guaymas hydrothermal vent systems. J. Moll. Stud. 85, 154–165. https://doi.org/10.1093/mollus/eyy061.
Matabos, M., Le Bris, N., Pendlebury, S., Thiébaut, E., 2008. Role of physico-chemical environment on gastropod assemblages at hydrothermal vents on the East Pacific Rise (13°N/EPR). J. Mar. Biol. Assoc. U. K. 88, 995–1008. https://doi.org/10.1017/S002531540800163X.
Matabos, M., Plouviez, S., Hourdez, S., Desbruyères, D., Legendre, P., Warén, A., et al., 2011. Faunal changes and geographic crypticism indicate the occurrence of a biogeographic transition zone along the southern East Pacific Rise. J. Biogeogr. 38, 575–594. https://doi.org/10.1111/j.1365-2699.2010.02418.x.
Methou, P., Cueff-Gauchard, V., Michel, L.N., Gayet, N., Pradillon, F., Cambon-Bonavita, M.-A., 2023. Symbioses of alvinocaridid shrimps from the South West Pacific: no chemosymbiotic diets but conserved gut microbiomes. Environ. Microbiol. Rep. 15, 614–630. https://doi.org/10.1111/1758-2229.13201.
Mills, S.W., Mullineaux, L.S., Tyler, P.A., 2007. Habitat associations in gastropod species at East Pacific Rise hydrothermal vents (9°50′N). Biol. Bull. 212, 185–194. https://doi.org/10.2307/25066601.
Mitarai, S., Watanabe, H., Nakajima, Y., Shchepetkin, A.F., McWilliams, J.C., 2016. Quantifying dispersal from hydrothermal vent fields in the western Pacific Ocean. Proc. Natl. Acad. Sci. 113, 2976–2981. https://doi.org/10.1073/pnas.1518395113.
Moss, R., Scott, S.D., Binns, R.A., 2001. Gold content of eastern Manus Basin volcanic rocks: implications for enrichment in associated hydrothermal precipitates. Econ. Geol. 96, 91–107. https://doi.org/10.2113/gsecongeo.96.1.91.
Mottl, M.J., Seewald, J.S., Wheat, C.G., Tivey, M.K., Michael, P.J., Proskurowski, G., et al., 2011. Chemistry of hot springs along the Eastern Lau Spreading Center. Geochim. Cosmochim. Acta 75, 1013–1038. https://doi.org/10.1016/j.gca.2010.12.008.
Mullineaux, L.S., Fisher, C.R., Peterson, C.H., Schaeffer, S.W., 2000. Tubeworm succession at hydrothermal vents: use of biogenic cues to reduce habitat selection error? Oecologia 123, 275–284. https://doi.org/10.1007/s004420051014.
Mullineaux, L.S., Peterson, C.H., Micheli, F., Mills, S.W., 2003. Successional mechanism varies along a gradient in hydrothermal fluid flux at deep-sea vents. Ecological monographs 73, 523–542. https://doi.org/10.1890/02-0674.
Mullineaux, L.S., Metaxas, A., Beaulieu, S.E., Bright, M., Gollner, S., Grupe, B.M., et al., 2018. Exploring the ecology of deep-sea hydrothermal vents in a metacommunity framework. Front. Mar. Sci. 5, 49. https://doi.org/10.3389/fmars.2018.00049.
Nakagawa, S., Takai, K., 2008. Deep-sea vent chemoautotrophs: diversity, biochemistry and ecological significance. FEMS Microbiol. Ecol. 65, 1–14. https://doi.org/10.1111/j.1574-6941.2008.00502.x.
Oksanen, J., Simpson, G.L., Blanchet, F.G., Kindt, R., Legendre, P., Minchin, P.R., et al., 2022. vegan: Community Ecology Package. Available at: https://CRAN.R-project.org/package=vegan. (Accessed 7 June 2022).
Pearson, K.A.M., Rouse, G.W., 2022. Vampire Worms; a revision of *Galapagomystides* (Phyllodocidae, Annelida), with the description of three new species. Zootaxa 5128, 451–485. https://doi.org/10.11646/zootaxa.5128.4.1.
Pelleter, E., Fouquet, Y., Etoubleau, J., Cheron, S., Labanieh, S., Josso, P., et al., 2017. Ni-Cu-Co-rich hydrothermal manganese mineralization in the Wallis and Futuna back-

arc environment (SW Pacific). Ore Geol. Rev. 87, 126–146. https://doi.org/10.1016/j.oregeorev.2016.09.014.
Peres-Neto, P.R., Legendre, P., Dray, S., Borcard, D., 2006. Variation partitioning of species data matrices: estimation and comparison of fractions. Ecology 87, 2614–2625. https://doi.org/10.1890/0012-9658(2006)87[2614:VPOSDM]2.0.CO;2.
Plouviez, S., Shank, T.M., Faure, B., Daguin-Thiébaut, C., Viard, F., Lallier, F.H., et al., 2009. Comparative phylogeography among hydrothermal vent species along the East Pacific Rise reveals vicariant processes and population expansion in the South. Mol. Ecol. 18, 3903–3917. https://doi.org/10.1111/j.1365-294X.2009.04325.x.
Plouviez, S., LaBella, A.L., Weisrock, D.W., Von Meijenfeldt, F.A.B., Ball, B., Neigel, J.E., et al., 2019. Amplicon sequencing of 42 nuclear loci supports directional gene flow between South Pacific populations of a hydrothermal vent limpet. Ecol. Evol. 9, 6568–6580. https://doi.org/10.1002/ece3.5235.
Podani, J., Schmera, D., 2011. A new conceptual and methodological framework for exploring and explaining pattern in presence – absence data. Oikos 120, 1625–1638. https://doi.org/10.1111/j.1600-0706.2011.19451.x.
Podani, J., Ricotta, C., Schmera, D., 2013. A general framework for analyzing beta diversity, nestedness and related community-level phenomena based on abundance data. Ecol. Complex. 15, 52–61. https://doi.org/10.1016/j.ecocom.2013.03.002.
Podowski, E.L., Moore, T.S., Zelnio, K.A., Luther, G.W., Fisher, C.R., 2009. Distribution of diffuse flow megafauna in two sites on the Eastern Lau Spreading Center, Tonga. Deep Sea Res. Part Oceanogr. Res. Pap. 56, 2041–2056. https://doi.org/10.1016/j.dsr.2009.07.002.
Podowski, E.L., Ma, S., Luther, G.W., Wardrop, D., Fisher, C.R., 2010. Biotic and abiotic factors affecting distributions of megafauna in diffuse flow on andesite and basalt along the Eastern Lau Spreading Center, Tonga. Mar. Ecol. Prog. Ser. 418, 25–45. https://doi.org/10.3354/meps08797.
Poitrimol, C., Thiébaut, É., Daguin-Thiébaut, C., Port, A.-S., Ballenghien, M., Tran Lu Y, A., et al., 2022. Contrasted phylogeographic patterns of hydrothermal vent gastropods along South West Pacific: Woodlark Basin, a possible contact zone and/or stepping-stone. PloS One 17, e0275638. https://doi.org/10.1371/journal.pone.0275638.
R Core Team, 2020. R: A language and environment for statistical computing. Available at: https://www.R-project.org/.
Reeves, E.P., Seewald, J.S., Saccocia, P., Bach, W., Craddock, P.R., Shanks, W.C., et al., 2011. Geochemistry of hydrothermal fluids from the PACMANUS, Northeast Pual and Vienna Woods hydrothermal fields, Manus Basin, Papua New Guinea. Geochim. Cosmochim. Acta 75, 1088–1123. https://doi.org/10.1016/j.gca.2010.11.008.
Rouxel, O., Toner, B., Germain, Y., Glazer, B., 2018. Geochemical and iron isotopic insights into hydrothermal iron oxyhydroxide deposit formation at Loihi Seamount. Geochim. Cosmochim. Acta 220, 449–482. https://doi.org/10.1016/j.gca.2017.09.050.
RStudio Team, 2020. RStudio: integrated development for R. Available at: http://www.rstudio.com/.
Rudnicki, M.D., Elderfield, H., 1992. Helium, radon and manganese at the TAG and Snakepit hydrothermal vent fields, 26° and 23°N, Mid-Atlantic Ridge. Earth Planet. Sci. Lett. 113, 307–321. https://doi.org/10.1016/0012-821X(92)90136-J.
Sarrazin, J., Robigou, V., Juniper, S.K., Delaney, J.R., 1997. Biological and geological dynamics over four years on a high-temperature sulfide structure at the Juan de Fuca Ridge hydrothermal observatory. Mar. Ecol. Prog. Ser. 153, 5–24. https://doi.org/10.3354/meps153005.
Schellart, W.P., Lister, G.S., Toy, V.G., 2006. A Late Cretaceous and Cenozoic reconstruction of the Southwest Pacific region: tectonics controlled by subduction and slab rollback processes. Earth Sci. Rev. 76, 191–233. https://doi.org/10.1016/j.earscirev.2006.01.002.
Seewald, J.S., Reeves, E.P., Bach, W., Saccocia, P.J., Craddock, P.R., Shanks, W.C., et al., 2015. Submarine venting of magmatic volatiles in the Eastern Manus Basin, Papua New Guinea. Geochim. Cosmochim. Acta 163, 178–199. https://doi.org/10.1016/j.gca.2015.04.023.
Sen, A., Becker, E.L., Podowski, E.L., Wickes, L.N., Ma, S., Mullaugh, K.M., et al., 2013. Distribution of mega fauna on sulfide edifices on the Eastern Lau spreading center and Valu Fa Ridge. Deep Sea Res. Part Oceanogr. Res. Pap. 72, 48–60. https://doi.org/10.1016/j.dsr.2012.11.003.
Shank, T.M., Fornari, D.J., Von Damm, K.L., Lilley, M.D., Haymon, R.M., Lutz, R.A., 1998. Temporal and spatial patterns of biological community development at nascent deep-sea hydrothermal vents (9°50′N, East Pacific Rise). Deep Sea Res. Part II Top. Stud. Oceanogr. 45, 465–515. https://doi.org/10.1016/S0967-0645(97)00089-1.
Socolar, J.B., Gilroy, J.J., Kunin, W.E., Edwards, D.P., 2016. How should beta-diversity inform biodiversity conservation? Trends Ecol. Evol. 31, 67–80. https://doi.org/10.1016/j.tree.2015.11.005.
Thaler, A.D., Zelnio, K., Saleu, W., Schultz, T.F., Carlsson, J., Cunningham, C., et al., 2011. The spatial scale of genetic subdivision in populations of *Ifremeria nautilei*, a hydrothermal-vent gastropod from the southwest Pacific. BMC Evol. Biol. 11, 372. https://doi.org/10.1186/1471-2148-11-372.
Thaler, A.D., Plouviez, S., Saleu, W., Alei, F., Jacobson, A., Boyle, E.A., et al., 2014. Comparative population structure of two deep-sea hydrothermal-vent-associated decapods (*Chorocaris* sp. 2 and *Munidopsis lauensis*) from Southwestern Pacific back-arc basins. PloS One 9, e101345. https://doi.org/10.1371/journal.pone.0101345.
Tran Lu Y, A., Ruault, S., Daguin-Thiébaut, C., Castel, J., Bierne, N., Broquet, T., et al., 2022. Subtle limits to connectivity revealed by outlier loci within two divergent metapopulations of the deep-sea hydrothermal gastropod *Ifremeria nautilei*. Mol. Ecol. 31, 2796–2813. https://doi.org/10.1111/mec.16430.
Tran Lu Y, A., Ruault, S., Daguin-Thiébaut, C., Le Port, A.-S., Ballenghien, M., Castel, J., et al., 2025. Comparative population genomics unveils congruent secondary suture zone in Southwest Pacific hydrothermal vents. Mol. Biol. Evol.doi. https://doi.org/10.1093/molbev/msaf024.
Tunnicliffe, V., 1991. The biology of hydrothermal vents: ecology and evolution. Oceanogr. Mar. Biol. 29, 319–407.
Tunnicliffe, V., Chen, C., Giguère, T., Rowden, A.A., Watanabe, H.K., Brunner, O., 2024. Hydrothermal vent fauna of the western Pacific Ocean: distribution patterns and biogeographic networks. Divers. Distrib. 30, e13794. https://doi.org/10.1111/ddi.13794.
Van Audenhaege, L., Matabos, M., Brind'Amour, A., Drugmand, J., Laës-Huon, A., Sarradin, P.-M., et al., 2022. Long-term monitoring reveals unprecedented stability of a vent mussel assemblage on the Mid-Atlantic Ridge. Prog. Oceanogr. 204, 102791. https://doi.org/10.1016/j.pocean.2022.102791.
Van Dover, C.L., 2000. The Ecology of Deep-sea Hydrothermal Vents. Princeton University Press. https://doi.org/10.1515/9780691239477.
Van Dover, C.L., 2002. Evolution and biogeography of deep-sea vent and seep invertebrates. Science 295, 1253–1257. https://doi.org/10.1126/science.1067361.
Vismann, B., 1991. Sulfide tolerance: physiological mechanisms and ecological implications. Ophelia 34, 1–27. https://doi.org/10.1080/00785326.1991.10429703.
Von Damm, K.L., 1990. Seafloor hydrothermal activity: black smoker chemistry and chimneys. Annu. Rev. Earth Planet. Sci. 18, 173–204. https://doi.org/10.1146/annurev.ea.18.050190.001133.
Vuillemin, R., Le Roux, D., Dorval, P., Bucas, K., Sudreau, J.P., Hamon, M., et al., 2009. CHEMINI: a new in situ CHEmical MINIaturized analyzer. Deep Sea Res. Part Oceanogr. Res. Pap. 56, 1391–1399. https://doi.org/10.1016/j.dsr.2009.02.002.
Watanabe, H.K., Shigeno, S., Fujikura, K., Matsui, T., Kato, S., Yamamoto, H., 2019. Faunal composition of deep-sea hydrothermal vent fields on the Izu–Bonin–Mariana Arc, northwestern Pacific. Deep Sea Res. Part Oceanogr. Res. Pap. 149, 103050. https://doi.org/10.1016/j.dsr.2019.05.010.
Whittaker, R.H., 1960. Vegetation of the Siskiyou Mountains, Oregon and California. Ecological monographs 30, 279–338. https://doi.org/10.2307/1943563.
Whittaker, R.H., 1972. Evolution and measurement of species diversity. Taxon 21, 213–251. https://doi.org/10.2307/1218190.
Zhang, D., Zhou, Y., Yen, N., Hiley, A.S., Rouse, G.W., 2023. *Ophryotrocha* (Dorvilleidae, Polychaeta, Annelida) from deep-sea hydrothermal vents, with the description of five new species. Eur. J. Taxon. 864, 167–194. https://doi.org/10.5852/ejt.2023.864.2101.